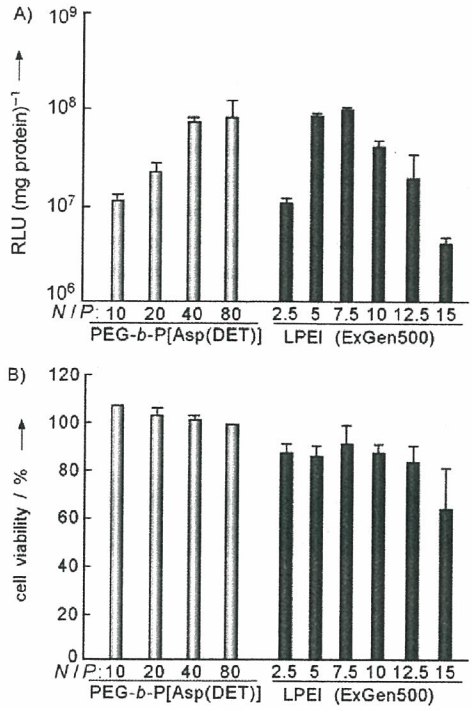

Figure 9. A) In vitro transfection efficiency and B) cytotoxicity of the PEG-*b*-P[Asp(DET)] polyplex micelles and LPEI polyplexes with varying *N/P* ratios toward mouse primary osteoblasts after a 48 h incubation.

Thus, we have successfully obtained highly transfection-efficient and less toxic polyplex micelles in this study. Particularly, the less toxic nature of the block catiomers compared with conventional catiomers of high transfection efficiency, as observed in Figure 8, should be of great significance for in vivo nonviral gene therapy. Indeed, bone regeneration in critical-size cranial defects based on in vivo transduction of osteogenic factors was recently carried out by our research group by using the PEG-*b*-P[Asp(DET)] polyplex micelle with plasmids expressing the optimized combination of osteogenic factors to facilitate cellular differentiation in situ.[18] Furthermore, polyplex micelles with the PEG palisade seem to be suitable for systemic gene delivery,[7,11] and the engineering the constituent block catiomers to construct polyplex micelles with integrated smart functions such as environment sensitivity[8,10] and tissue targetability[9] will maximize the efficacy of nonviral gene therapy. Thus, the PEG-*b*-P[Asp(DET)] polyplex micelle is expected to be a biocompatible vector system applicable toward various aspects of gene medicine.

Conclusion

We have established a simple and novel synthetic route for the generation of biocompatible block catiomers through the quantitative aminolysis of PEG-*b*-PBLA. The construction of a library of block catiomers, the PEG-*b*-polyaspartamides carrying a series of amine compounds in the side chain, revealed the importance of the ethylenediamine unit for enhanced and less toxic gene transfection by the polyplex micelles made from pDNA and the block catiomers. The availability of the polyplex micelles developed in this study for the transfection of primary osteoblasts will facilitate the use of this type of block catiomer for the construction of synthetic vectors suitable for nonviral gene therapy.

Experimental Section

Materials: β-Benzyl-L-aspartate *N*-carboxyanhydride (BLA-NCA) and α-methoxy-ω-amino poly(ethylene glycol) (MeO-PEG-NH_2) (M_r = 12000) were obtained from Nippon Oil and Fats (Tokyo, Japan). Ethylenediamine (EDA), diethylenetriamine (DET) and 4-methyldiethylenetriamine (MDET) were purchased from Tokyo Kasei Kogyo (Tokyo, Japan) and distilled over CaH_2 under decreased pressure. *N,N*-Diethyldiethylenetriamine (DEDET) was purchased from Lancaster Synthesis, (Lancashire, England) and distilled over CaH_2 under decreased pressure. *N,N*-Dimethylformamide (DMF), dichloromethane, and acetic anhydride were purchased from Wako Pure Chemical Industries, (Osaka, Japan) and purified by general methods before use.

Synthesis of PEG-*b*-polyaspartamide catiomers: The PEG-*block*-poly(β-benzyl L-aspartate) (PEG-*b*-PBLA) copolymer was prepared as previously reported.[19] Briefly, BLA-NCA was polymerized in DMF at 40 °C by the initiation from the terminal primary amino group of MeO-PEG-NH_2, followed by acetylation of the *N*-terminus of PBLA to obtain PEG-*b*-PBLA. PEG-*b*-PBLA was confirmed to have a unimodal molecular weight distribution (M_w/M_n: 1.17) by gel-permeation chromatography (GPC) measurement (columns: TSK-gel G4000HHR + G3000HHR, eluent: DMF + 10 mM LiCl, T = 40 °C, detector: RI) (data not shown). The degree of polymerization (DP) of PBLA was calculated to be 68 based on ^{1}H NMR spectroscopy (data not shown).

Lyophilized PEG-*b*-PBLA (300 mg, 11.6 μmol) was dissolved in DMF (10 mL), followed by reaction with DET (50 equiv to benzyl group of PBLA segment, 4.0 g, 39.4 mmol) under mild anhydrous conditions at 40 °C to obtain PEG-*b*-P[Asp(DET)]. After 24 h, the reaction mixture was slowly added dropwise into a solution of acetic acid (10% *v/v*, 40 mL) and dialyzed against a solution of 0.01 N HCl and distilled water (M_r cutoff: 3500 Da). The final solution was lyophilized to obtain the polymer as the chloride salt form, and the yield was approximately 90%. Similarly, other block catiomers, PEG-*b*-P[Asp(EDA)], PEG-*b*-P[Asp(MDET)], and PEG-*b*-P[Asp(DEDET)] were synthesized by the aminolysis reaction of PEG-*b*-PBLA with EDA, MDET, and DEDET, respectively. The structures of these block catiomers were confirmed by ^{1}H and ^{13}C NMR measurements and size-exclusion chromatography (SEC).

Potentiometric titration of block catiomers: PEG-*b*-P[Asp(DET)] (30 mg) was dissolved in 50 mL 0.01 N HCl and titrated with 0.01 N NaOH. An automatic titrator (TS-2000, Hiranuma, Kyoto, Japan) was used for titration. In this experiment, the titrant was added in quantities of 0.063 mL after the pH values were stabilized (minimal interval: 30 s). The α/pH curves were determined from the obtained titration curves.

Dye exclusion assay: Polyplex solutions with a pDNA concentration of 33 μg mL^{-1}, prepared by mixing pDNA and block catiomers at different *N/P* ratios (*N* = total amines in block catiomer; *P* = total phosphate anions in pDNA), were diluted to 10 μg pDNA mL^{-1} with ethidium bromide (EtBr, 2.5 mg mL^{-1}) in 10 mM Tris–HCl (pH 7.4) or 10 mM sodium acetate (pH 5.0) buffer. The sample solutions were incubated at ambient temperature overnight. The fluo-

rescence intensity of the samples at $\lambda = 590$ nm (excitation at $\lambda = 510$ nm) was measured at 25 °C with a spectrofluorometer (FP-6500, Jasco, Tokyo, Japan). The relative fluorescence intensity was calculated as: $F_r = (F_{sample} - F_0)/(F_{100} - F_0)$, for which F_{sample}, F_{100}, and F_0 represent the fluorescence intensity of the samples, free pDNA, and background, respectively.

Dynamic light scattering (DLS) and ζ potential measurements: In the DLS measurements, polyplex solutions with various *N/P* ratios in 10 mM Tris–HCl buffer (pH 7.4) were adjusted to have pDNA concentrations of 33.3 μg mL^{-1}. DLS measurements were then performed at 25 ± 0.2 °C with a DLS-7000 instrument (Otsuka Electronics, Osaka, Japan) with a vertically polarized incident beam of $\lambda = 488$ nm from an Ar ion laser. The ζ potential of the polyplex micelles was measured at 25 ± 0.2 °C with an ELS-6000 instrument (Otsuka Electronics, Osaka, Japan) equipped with a He–Ne ion laser ($\lambda = 633$ nm). The scattering angle was fixed at 20°. From the obtained electrophoretic mobility, the ζ potential was calculated by using the Smoluchowski equation: $\zeta = 4\pi\eta\upsilon/\varepsilon$ in which η is the electrophoretic mobility, υ is the viscosity of the solvent, and ε is the dielectric constant of the solvent. The results are expressed as the average of five experiments.

In vitro transfection of HuH-7 cells: Human hepatoma HuH-7 cells were seeded on 6-well culture plates and incubated overnight in 1.5 mL Dulbecco's modified Eagle medium (DMEM) containing 10% fetal bovine serum (FBS) before transfection. The cells were then incubated with the polyplex micelles from PEG-*b*-P[Asp(EDA)], PEG-*b*-P[Asp(DET)], PEG-*b*-P[Asp(MDET)], and PEG-*b*-P[Asp(DEDET)] (3 μg pDNA/well) with various *N/P* ratios in DMEM containing 10% FBS for 24 h, followed by an additional incubation for 24 h in the absence of polyplexes. Luciferase gene expression was evaluated using the Luciferase Assay System (Promega, Madison, USA) and a Lumat LB9507 luminometer (Berthold Technologies, Bad Wildbad, Germany). The results were expressed as light units per milligram of cell protein determined by a BCA assay kit (Pierce, Rockford, USA).

Mouse primary osteoblast culture and transfection: Osteoblasts were isolated from calvariae of neonatal littermates. The experimental procedures were handled in accordance with the guidelines of the Animal Committee of the University of Tokyo. Calvariae were digested for 10 min at 37 °C in an enzyme solution containing 0.1% collagenase and 0.2% dispase for five cycles. Cells isolated by the final four digestions were combined as an osteoblast population and cultured in DMEM containing 10% FBS. For luciferase transfection assays, primary osteoblasts were inoculated at a density of 2×10^4 cells/well in a 24-multiwell plate, cultured for 24 h, and, after changing to fresh culture medium containing 10% FBS, pDNA polyplex solution (33.3 μg mL^{-1}, 22.5 μL) was applied to each well. Luciferase gene expression was measured 48 h later by using the Luciferase Assay System (Promega) and a Lumat LB9507 luminometer (Berthold). For the cytotoxicity assay, primary osteoblasts were plated into a 96-multiwell plate (6×10^3 cells/well). After 24 h incubation, 6 μL of each pDNA polyplex solution was added, followed by further incubation for 24 h. The viability of the cells was evaluated by an MTT assay (Cell Counting Kit-8, Dojindo, MTT = 3-[4,5-dimethylthiazol-2-yl]-2,5-diphenyltetrazolium bromide). Each well was measured by reading the absorbance at $\lambda = 450$ nm according to the protocol provided by the manufacturer.

Acknowledgements

The authors are grateful to the Health and Labor Sciences Research Grants in Research on Advanced Medical Technology in Nanomedicine Area from the Ministry of Health, Labor and Welfare (MHLW), Japan. They also express their thanks for the Grant-in-Aid for Scientific Research, the Special Coordination Funds for Promoting Science and Technology, and the Project on the Materials Development for Innovative Nano-Drug Delivery Systems from the Ministry of Education, Culture, Sports, Science and Technology (MEXT), Japan. The authors thank Professor Yukio Nagasaki and Dr. Motoi Oishi (University of Tsukuba) for use of the SEC instruments and their helpful suggestions, and Mr. Masataka Nakanishi for valuable discussions.

Keywords: aminolysis · block copolymers · gene delivery · polycations · polymeric micelles

[1] I. M. Verma, N. Somia, *Nature* **1997**, *389*, 239.
[2] M. Ogris, E. Wagner, *Drug Discovery Today* **2002**, *7*, 479.
[3] A. K. Salem, P. C. Searson, K. W. Leong, *Nat. Mater.* **2003**, *2*, 668.
[4] N. Nishiyama, A. Iriyama, W.-D. Jang, K. Miyata, K. Itaka, Y. Inoue, H. Takahashi, Y. Yanagi, Y. Tamaki, H. Koyama, K. Kataoka, *Nat. Mater.* **2005**, *4*, 934.
[5] S. O. Han, R. I. Mahato, S. W. Kim, *Bioconjugate Chem.* **2001**, *12*, 337.
[6] Y. Liu, L. Wenning, M. Lynch, T. M. Reineke, *J. Am. Chem. Soc.* **2004**, *126*, 7422.
[7] K. Itaka, K. Yamauchi, A. Harada, K. Nakamura, H. Kawaguchi, K. Kataoka, *Biomaterials* **2003**, *24*, 4495.
[8] K. Miyata, Y. Kakizawa, N. Nishiyama, A. Harada, Y. Yamasaki, H. Koyama, K. Kataoka, *J. Am. Chem. Soc.* **2004**, *126*, 2355.
[9] D. Wakebayashi, N. Nishiyama, Y. Yamasaki, K. Itaka, N. Kanayama, A. Harada, Y. Nagasaki, K. Kataoka, *J. Controlled Release* **2004**, *95*, 653.
[10] S. Fukushima, K. Miyata, N. Nishiyama, N. Kanayama, Y. Yamasaki, K. Kataoka, *J. Am. Chem. Soc.* **2005**, *127*, 2810.
[11] M. Harada-Shiba, K. Yamauchi, A. Harada, I. Takamisawa, K. Shimokado, K. Kataoka, *Gene Ther.* **2002**, *9*, 407.
[12] Y.-Y. Kim, H.-C. Chang, Y. T. Lee, U.-I. Cho, D. W. Boo, *J. Phys. Chem. A* **2003**, *107*, 5007.
[13] J.-P. Behr, *Chemia* **1997**, *51*, 34.
[14] V. Saudek, H. Pivcova, J. Drobnik, *Biopolymers* **1981**, *20*, 1615.
[15] A. V. Kabanov, T. K. Bronich, V. A. Kabanov, K. Yu, A. Eisenberg, *Macromolecules* **1996**, *29*, 6797.
[16] R. T. Franceschi, S. Yang, R. B. Rutherford, P. H. Krebsbach, M. Zhao, D. Wang, *Cells Tissues Organs* **2004**, *176*, 95 – 108.
[17] C. L. Gebhart, A. V. Kabanov, *J. Controlled Release* **2001**, *73*, 401.
[18] K. Itaka, N. Kanayama, N. Nishiyama, S. Fukushima, Y. Yamasaki, S. Oba, U.-I. Chung, H. Kawaguchi, K. Nakamura, K. Kataoka, *Proceedings of the 12th International Symposium on Recent Advances in Drug-Delivery Systems and CRS Winter Symposium, Salt Lake City, Utah, USA, February 21 – 24*, **2005**, 9.
[19] A. Harada, K. Kataoka, *Macromolecules* **1995**, *28*, 5294.

Received: December 21, 2005
Published online on February 24, 2006

CLINICAL ORTHOPAEDICS AND RELATED RESEARCH
Number 453, pp. 58–63

2006 FRANK STINCHFIELD AWARD

Grafting of Biocompatible Polymer for Longevity of Artificial Hip Joints

Toru Moro, MD; Yoshio Takatori, MD*; Kazuhiko Ishihara, PhD†; Kozo Nakamura, MD*; and Hiroshi Kawaguchi, MD**

Aseptic loosening induced by wear particles from the polyethylene liner is likely the most common cause of long-term total hip arthroplasty failure. We developed a novel hip polyethylene liner with the surface graft of a biocompatible phospholipid polymer, 2-methacryloyloxyethyl phosphorylcholine (MPC), and previously reported the grafting decreased the short-term production of wear particles and the subsequent bone resorptive responses. For clinical application, we investigated the stability of the 2-methacryloyloxyethyl phosphorylcholine grafting during sterilization and the wear resistance of the sterilized liner during longer loading comparable to clinical usage. Radiographic spectroscopy confirmed the stability of the 2-methacryloyloxyethyl phosphorylcholine polymer on the liner surface after the gamma irradiation. We used a hip wear simulator up to 1×10^7 cycles to test sterilized cross-linked polyethylene liners with and without 2-methacryloyloxyethyl phosphorylcholine grafting. The 2-methacryloyloxyethyl phosphorylcholine grafting markedly decreased the friction, the production of wear particles, and the wear of the liner surface. These data suggest a marked improvement in the wear resistance of the polyethylene liner by the 2-methacryloyloxyethyl phosphorylcholine grafting for clinically relevant periods after sterilization, indicating 2-methacryloyloxyethyl phosphorylcholine grafting is a promising technology for extending longevity of artificial hips.

From the *Department of Sensory & Motor System Medicine, Faculty of Medicine; and the †Department of Materials Engineering, School of Engineering, The University of Tokyo, Tokyo, Japan.
One or more of the authors has received funding from grants-in-Aid for Scientific Research from the Japanese Ministry of Education, Culture, Sports, Science and Technology (#15390449) (YT), and Health and Welfare Research Grant for Translational Research from the Japanese Ministry of Health, Labour and Welfare (KN).
Correspondence to: Toru Moro, MD, PhD, Department of Sensory & Motor System Medicine, Faculty of Medicine, The University of Tokyo, Hongo 7-3-1, Bunkyo, Tokyo 113-0033, Japan. Phone: 81-3-5800-8656; Fax: 81-3-3818-4082; E-mail: moro-ort@h.u-tokyo.ac.jp.
DOI: 10.1097/01.blo.0000246553.33434.5f

The incidence of osteoarthritis (OA) is on the rise because of the worldwide growth of elderly populations. Total hip arthroplasty (THA) is one of the most successful and effective treatments for patients with end-stage arthritic diseases of the hip.[4,37] The number of primary THAs performed annually is estimated to be more than 1.3 million worldwide, with 50 to 140 operations per 100,000 inhabitants in North America, Europe, and Australia. This rate is expected to continue to increase over at least the next three decades.[1,25,33] Despite improvements in implant design and surgical technique, aseptic loosening of artificial joints caused by periprosthetic osteolysis is the most common problem limiting implant survivorship and clinical success.[21] However, there is no treatment for painful loosening other than the revision surgery, and the number of salvage operations with outcomes poorer than the primary procedures is increasing.[29]

The pathogenesis of the periprosthetic osteolysis is a consequence of the host inflammatory response to wear particles from prosthetic devices.[21] The most abundant and bone resorptive particle within the periprosthetic tissue is polyethylene (PE) generated from the interface between PE and metal components.[30] Polyethylene particles induce phagocytosis by macrophages and subsequently secretion of bone resorptive cytokines.[9] Therefore, there are two approaches to prevent aseptic loosening: reduce the amount of PE wear particles or suppress the subsequent bone resorptive responses. Studies have been performed to increase the wear resistance of PE or to develop alternative bearing surfaces other than PE, but none has fully solved the problem.

The surface of healthy human articular cartilage is covered with a nanometer-scaled phospholipid layer that improves the lubricity and biocompatibility of the articulating surface.[13,24] Therefore, grafting a polymer including the biocompatible phospholipid-like layer on an artificial liner surface may replicate interface conditions similar to a healthy joint. The 2-methacryloyloxyethyl phosphoryl-

choline (MPC) polymer, the natural biocompatible polymer, has a side chain composed of phosphorylcholine resembling phospholipids of biomembrane (Fig 1).[20] The MPC grafting onto the surface of other medical devices suppresses biological reactions when they are in contact with living organisms,[19,42] and is now clinically used on the surfaces of intravascular stents, intravascular guide wires, soft contact lenses, and the artificial lung authorized by the United States Food and Drug Administration.[23,27]

To reduce wear particles and eliminate periprosthetic osteolysis, we prepared a novel PE hip liner with MPC grafted onto its surface. Our previous study suggests grafted MPC decreases the production of wear particles and secretion of cytokines and osteoclastogenesis during a brief period of 3×10^6 cycles in a hip wear simulator.[34] However, the effect of the sterilization procedure on the stability of the MPC grafting and the wear resistance of the sterilized liner during longer loading comparable to clinical usage remains to be elucidated before clinical application.

We evaluated MPC stability after sterilization and the wear resistance of the sterilized MPC-grafted PE liner during longer loading comparable to clinical usage.

MATERIALS AND METHODS

We used a hip simulator to investigate the MPC stability after sterilization and the wear resistance of the sterilized MPC-grafted PE liner during 1×10^7 cycles of loading, comparable to 10 to 30 years of walking. The stability of the MPC polymer on MPC-CLPE plate after the gamma irradiation was verified using the xray photoelectron spectroscopy (XPS) analysis, the Fourier transform infrared spectroscopic (FTIR) analysis, and the contact angle of a water drop. Mechanical effects of the MPC grafting on the hip prosthesis were examined using a hip wear simulator[22] under the conditions recommended by the International Organization for Standardization.

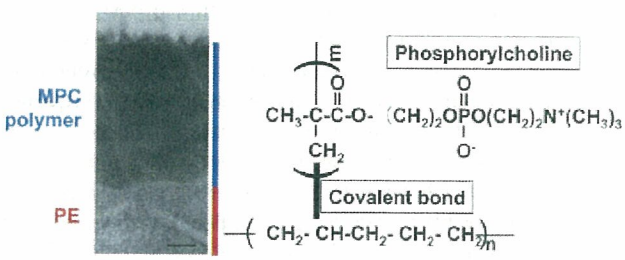

Fig 1. The MPC polymer is grafted onto the cross-linked polyethylene liner surface. A TEM image (left) shows the cross-linked PE liner surface grafted with MPC polymer stained black with ruthenium oxide show (scale bar, 20 nm). The chemical structure (right) of MPC and cross-linked PE is shown. 2-methacryloyloxyethyl phosphorylcholine is a biocompatible polymer with side chain composed of phosphorylcholine and resembles phospholipid of biomembrane. MPC is bound to the cross-linked PE liner by the covalent bond with a photoinduced graft polymerization technique.

We synthesized and purified MPC as previously reported (Fig 1).[20] We used cross-linked PE liner (K-MAX Excellink®, Japan Medical Materials, Osaka, Japan) and cobalt-chromium-molybdenum alloy femoral heads (K-MAX® HH-02, Japan Medical Materials). Grafting of the MPC polymer onto the surfaces of the cross-linked PE liner was performed using a photo-induced polymerization technique.[16,34] Briefly, cross-linked PE liners were placed in the MPC solution (0.5 mol/L) and photo-induced polymerization on the liner surface was performed using an ultra-high pressure mercury lamp (UVL-400HA, Riko-Kagaku Sangyo Co Ltd, Chiba, Japan).

To evaluate the influence of sterilization procedure, MPC-grafted cross-linked PE plates (MPC-CLPE plates) were sterilized with gamma irradiation (2.5 Mrad) in nitrogen as conventionally used. Elemental analysis at the surface was performed with a highly sensitive XPS (PHI5400MC, Perkin Elmer, Inc, Wellesley, MA), a FTIR (Perkin-Elmer FT-IR 1650, Perkin Elmer, Inc), and a transmission electron microscope (JEM-1010 Japan Electron Optics Laboratory Co, Ltd, Tokyo, Japan). The contact angle of water on the cross-linked PE surface was measured by the sessile drop method at room temperature (22°C) using a goniometer (Erma G-1, Tokyo, Japan).[18] At least 10 contact angles were measured and averaged.

A 12-station hip simulator apparatus (MTS, MTS Systems Co Ltd, Minneapolis, MN) with two types of gamma-sterilized cross-linked PE liners in 46 mm acetabular cups, a cross-linked PE liner and an MPC-grafted cross-linked PE liner (MPC-CLPE liner), coupled to 26 mm cobalt-chromium-molybdenum alloy heads were mounted on the rotating blocks to produce a biaxial or orbital motion. Friction torque between the liner and the femoral head was measured using a torque measuring instrument. We then applied a loading profile that simulated walking with continuous cyclic motion and loading (maximum force, 2744 N; frequency, 1 Hz).[38] A diluted bovine calf serum (25%) in distilled water was used as the lubricant. Sodium azide (10 mL/L) and ethylenediaminetetraacetic acid (20 mm) were added to prevent microbial contamination and minimize calcium phosphate formation on the implant surface. The simulator was run up to 1×10^7 cycles for 8 months. At intervals of 5×10^5 cycles the liners were removed from the simulator and weighed on a microbalance (Sartorius GENIUS ME215S, Sartorius AG, Göttingen, Germany). The lubricant was collected and stored at –20°C for further analysis. After total loading, microdamage of the liner surface was measured with a three-dimensional coordinate measuring machine (XYZAX GS800B, Tokyo Seimitsu Co, Ltd, Tokyo, Japan). To evaluate true removal of material caused by wear, melt-recovery experiments were performed and the liner surface was analyzed with confocal scanning laser microscope (OLS1200, Olympus Corp, Tokyo, Japan) as previously reported.[35] For the femoral head surface, in addition to scanning electron microscopy (SEM) evaluation, the surface roughness value R_a was measured using a roughness measuring instrument (SURFTEST-501, Mitsutoyo Co, Ltd, Kanagawa, Japan) with a 5 μm diameter contact probe. For the isolation of wear particles after loading, the lubricant was incubated with 5 N NaOH solu-

tion to digest adhesive proteins that were degraded and precipitated. Collected particles underwent sequential filtrations as previously reported.[22] The size of particles was defined as the maximum dimensions by the SEM analysis.

We compared the means of CLPE and MPC-CLPE groups by analysis of variance and determined significance by post-hoc testing using Bonferroni's method.

RESULTS

The XPS signals indicating nitrogen atoms (N_{1s}) at 402 eV and phosphorus atoms (P_{2p}) at 135 eV, which are attributable to the phosphorylcholine group in the MPC unit, were observed on the MPC-CLPE plate after gamma irritation (Fig 2A). The FTIR transmittance absorption representing phosphate group (P-O) at 1240, 1080, and 970 cm^{-1}, and ketone group (C = O) at 1720 cm^{-1} also was observed after grafting and irradiation (Fig 2B). The contact angle of a water droplet on the MPC-CLPE plate was 12.3° ± 2.4°, whereas the contact angle of a water droplet of the original cross-linked PE plate was 89.9° ± 2.9° (Fig 2C), suggesting the hydrophobic cross-linked PE surface was kept covered with hydrophilic MPC polymer after the gamma irritation.

In the hip simulator study (Fig 3A) the average friction torque was approximately 80% lower in MPC-CLPE liners than in cross-linked PE liners (Fig 3B). The gravimetric analysis showed a total weight loss of 34.7 ± 2.5 mg in cross-linked PE liners after 1×10^7 cycles of loading (Fig 3C). In contrast, MPC-CLPE liners continued to gain weight, showing a total weight gain of 8.7 ± 1 mg, which may have been attributable to water absorption into the liner from the lubricant.

Three-dimensional morphometric analyses of MPC-CLPE liner surface revealed little or no detectable wear, while substantial wear was detected in cross-linked PE liners (Fig 4A). The confocal scanning laser microscopic analysis of the liner surface clearly revealed original machine marks on the MPC-CLPE liner surface, but they were completely obliterated from the cross-linked PE liner (Fig 4B). The XPS analysis also confirmed the remainder of the specific spectra of N_{1s} and P_{2p} on the MPC-CLPE liner surface after the loading (Fig 2A), indicating the MPC-CLPE grafting was maintained after loading 1×10^7 cycles. The femoral heads were free of visible scratches and the surface roughness expressed by the R_a values was similar before and after loading in both groups (R_a = 0.04 – 0.05 μm), suggesting there was no abrasive contamination with metal particles from the heads in the hip simulator (Fig 4C).

The SEM analysis of the wear particles isolated from the lubricants showed no difference in the particle shapes or sizes between cross-linked PE and MPC-CLPE liners. Most of the particles from both liners ranged from 0.1 μm to1 μm and were round or spindle-shaped (Fig 5).

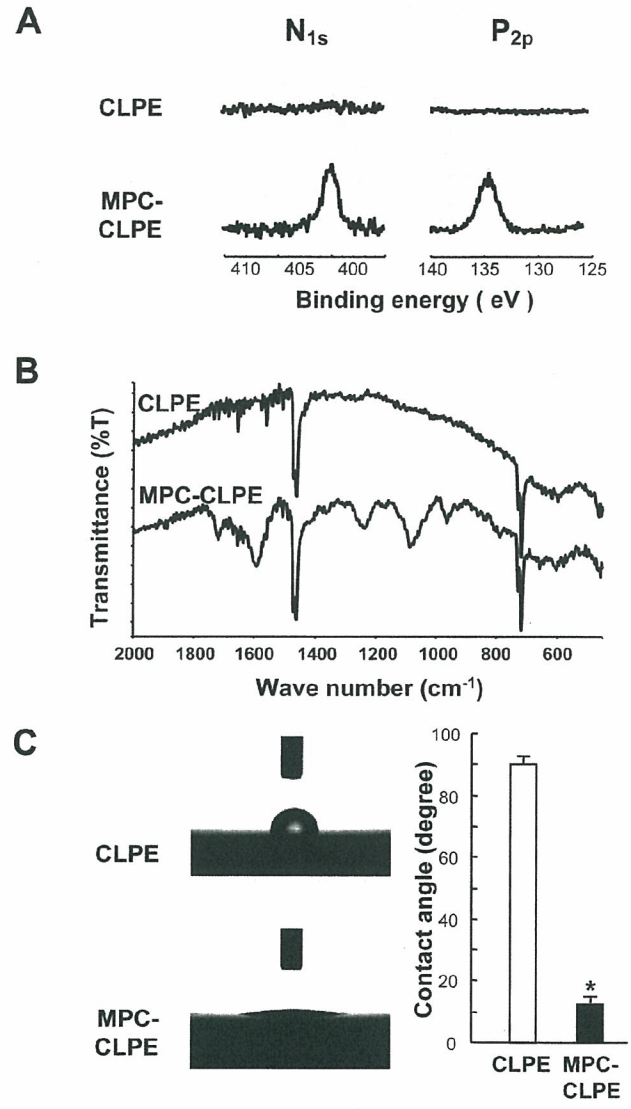

Fig 2A–C. (A) Xray photoelectron spectra of the cross-linked PE and MPC-CLPE plates after gamma sterilization are shown. The peaks in the nitrogen (N1s) and phosphorus (P2p) atom regions are specific to MPC, suggesting gamma sterilization did not affect the properties of MPC grafting. (B) Fourier transform infrared spectra of the cross-linked PE and MPC-CLPE plates after gamma sterilization are shown. Absorptions representing the phosphate group (P–O) at 1240, 1080, and 970 cm^{-1}, and ketone group (C = O) at 1720 cm^{-1} are also specific to MPC. (C) Hydrophilicity determined by the contact angle of a water drop with the cross-linked PE and MPC-CLPE plates after gamma sterilization is represented. Data are expressed as means (bars) ± standard errors (error bars) for 12 plates per group (*significant difference from cross-linked PE was set at $p < 0.01$).

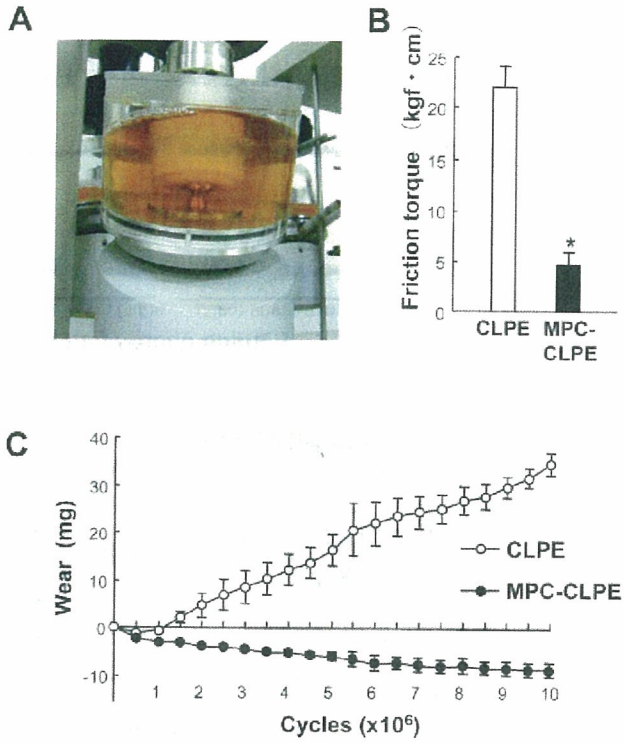

Fig 3A–C. (A) A photograph shows the hip simulator. (B) The bar graph shows friction torque of the cross-linked PE and MPC-CLPE liners against the femoral heads measured before the loading test. (C) The graph shows the time course of the amount of wear product from cross-linked PE and MPC-CLPE liners during 1×10^7 cycles of loading. Data are expressed as means (symbols and bars) ± standard errors (error bars) for 10 liners/group (*significant difference from cross-linked PE was set at $p < 0.01$).

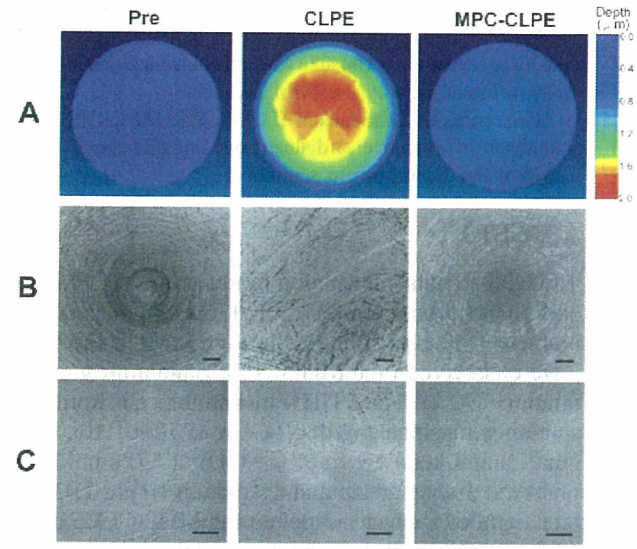

Fig 4A–C. (A) Three-dimensional morphometric analysis and (B) confocal scanning laser microscopic analysis of the liner surfaces before (pre) and after 1×10^7 cycles of loading on cross-linked PE and MPC-CLPE liners is shown (scale bars, 200 μm). (C) Scanning electron microscopy analyses of the femoral head surfaces before (pre) and after 1×10^7 cycles of loading showed the femoral heads were free of visible scratches in both liners (scale bars, 5 μm).

DISCUSSION

Our data suggest the biocompatible phospholipid polymer MPC grafted onto the PE liner surface of the hip prosthesis decreases friction and the production of wear particles during 1×10^7 cycles of loading in a hip simulator. Because PE particles are the most abundant and catabolic among wear particles in the periprosthetic tissues,[30] alternative bearing surfaces have been proposed such as ceramic-on-ceramic and metal-on-metal articulations; however, these have potential disadvantages.[2,3]

The major limitation of our study is the confined period of loading. Although the 1×10^7 cycles in the hip simulator is comparable to 10 to 30 years of physical walking, this may not be long enough for young active patients with aseptic necrosis or fracture. A hip simulator study with longer loading is now underway. Furthermore, a hip simulator does not entirely capture the range of loading conditions of a hip, in terms of either the variety of positions or the magnitude of loading. Nonetheless, we believe a simulator study can provide some indication of trends.

The long history and popularity of PE as a bearing surface has led to research in the development of tougher

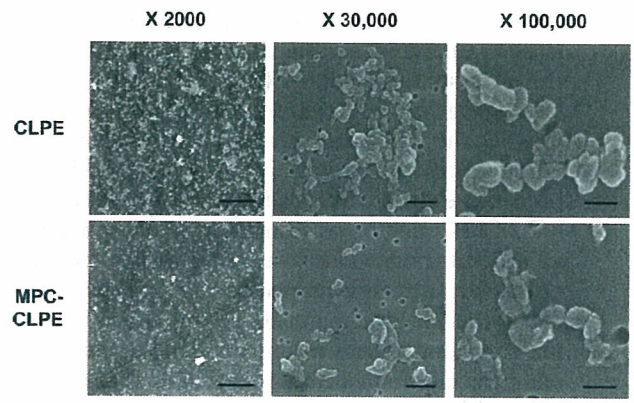

Fig 5. Scanning electron microscopy images show the wear particles isolated from lubricants of the simulators with cross-linked PE and MPC liners. Representative images are shown in three magnifications (×2000, ×30,000, and ×100,000; scale bars, 10 μm, 500 nm, and 200 nm, respectively).

and more wear-resistant PE materials. These include the incorporation of short chopped carbon fibers in PE matrix,[6,41] the extension of chain crystallite morphology with thicker lamellae and higher crystallinity,[28] and the creation of a three-dimensional molecular network by cross-linking. Of these, cross-linking improved the wear resistance and suppressed the periprosthetic osteolysis most efficiently in the clinical setting.[31] Grafting of MPC onto the cross-linked PE surface further increased the wear resistance over the conventional cross-linked PE.

Clinical and laboratory research suggests sterilization methods can dramatically affect the in vivo performance of PE liners.[32] Currently, PE liners can be sterilized with gamma irradiation, gas plasma, or ethylene oxide. Gamma sterilization in air has been shown to lead to oxidation of the PE and may adversely affect its mechanical properties. In the mid-1990s, the use of gamma sterilization in air was replaced by gamma sterilization in an inert environment, such as nitrogen, argon, or a vacuum. We used cross-linked PE liners sterilized gamma irradiation in nitrogen, and our data suggest this sterilization method did not affect the property of MPC grafting with respect to surface analysis and hip simulator study. Other MPC-grafted medical devices such as an oxygenator, intravascular stents, or intravascular guide wires are sterilized with gamma irradiation or ethylene oxide. Moreover, the MPC polymer has good thermal resistance and could be processed by heat treatment at 150°C. Our preliminary study showed gas plasma and ethylene oxide sterilization did not affect properties of the MPC polymer.[36]

Given a reduction of wear by the MPC grafting, we should consider the lubrication mechanism between the liners and metal heads. Although phospholipids work as effective boundary lubricants,[12,40] a study of natural synovial joints showed fluid film lubrication by the intermediate hydrated layer is the predominant mechanism under physiologic walking conditions.[7] Because we showed the MPC grafting onto the cross-linked PE plate increased hydrophilicity, and our previous study showed the free water fraction on the MPC polymer surface is kept at a higher level,[17] the reduction of wear is likely attributable to the hydrated lubricating layer formed by MPC grafting.

In addition to the improvement of the wear resistance of the liner, it is important to decrease bone resorptive responses induced by wear particles. Substantial differences between the wear particles from cross-linked and non-cross-linked PE liners have been found in vitro.[8,15] The cross-linked PE liner releases a relatively high number of submicrometer and nanometer-sized PE particles and relatively fewer particles that are several micrometers in dimension.[11] These submicrometer-sized PE particles induce a greater inflammatory response in vitro than larger particles.[15] Therefore, the biological activity of PE particles will depend on the total volume of wear or the number of particles generated and the proportion of those particles that are within the most biologically active size range.[8,11] In our previous study, MPC nanoparticles (500 nm in diameter) were used in a murine particle-induced osteolysis model to investigate the biocompatibility of these particles.[34] In vitro culture systems suggested MPC nanoparticles were not phagocytosed in substantial amounts by macrophages and do not induce the production of bone resorptive cytokines. Furthermore, the culture medium of macrophages exposed to MPC nanoparticles did not induce osteoclast formation from bone marrow cells. These results suggest MPC particles are biologically inert in respect to phagocytosis by macrophages and subsequent bone resorptive actions. An increasing number of studies address the potential pharmacologic modification of the adverse host response to wear particles,[5,10] including cytokine antagonists, cyclooxygenase-2 inhibitors, and osteoprotegerin, or anti-RANKL (receptor activator of nuclear vector kappa B ligand) antibody; however, they may cause serious side effects because the agents must taken for a long period after surgery and because they are not currently targeted to the site of the problem. Because the lack of side effects of the MPC polymer grafting has already been confirmed clinically by several biomaterials,[23,26] this grafting surpasses the developing pharmacologic treatments.

Although our study focused on the hip, MPC polymer grafting can be applicable to the prevention of periprosthetic osteolysis of other joints in which PE particles from articular interfaces between the PE and metal components are also thought to initiate the catabolic cascade.[14,39] From the advantages observed, we believe MPC polymer grafting will improve total joint replacement by preventing periprosthetic osteolysis and aseptic loosening. The development of this nanotechnology would improve the quality of care of patients having total joint replacement and have a substantial public health impact. We are currently designing a large-scale clinical trial.

Acknowledgments

We thank Tomohiro Konno, Noboru Yamawaki, Takatoshi Miyashita, Masayuki Kyomoto, Hiroaki Takadama, Kaori Jono, and Reiko Yamaguchi for their excellent technical help.

References

1. Birrell F, Johnell O, Silman A. Projecting the need for hip replacement over the next three decades: influence of changing demography and threshold for surgery. *Ann Rheum Dis*. 1999;58:569–572.
2. Black J. Metal on metal bearings. A practical alternative to metal on polyethylene total joints? *Clin Orthop Relat Res*. 1996;329: S244–S255.
3. Callaway GH, Flynn W, Ranawat CS, Sculco TP. Fracture of the femoral head after ceramic-on-polyethylene total hip arthroplasty. *J Arthroplasty*. 1995;10:855–859.

4. Charnley J. Total hip replacement by low-friction arthroplasty. *Clin Orthop Relat Res.* 1970;72:7–21.
5. Childs LM, Paschalis EP, Xing L, Dougall WC, Anderson D, Boskey AL, Puzas JE, Rosier RN, O'Keefe RJ, Boyce BF, Schwarz EM. In vivo RANK signaling blockade using the receptor activator of NF-kappaB:Fc effectively prevents and ameliorates wear debris-induced osteolysis via osteoclast depletion without inhibiting osteogenesis. *J Bone Miner Res.* 2002;17:192–199.
6. Connelly GM, Rimnac CM, Wright TM, Hertzberg RW, Manson JA. Fatigue crack propagation behavior of ultrahigh molecular weight polyethylene. *J Orthop Res.* 1984;2:119–125.
7. Dowson D, Jin ZM. Micro-elastohydrodynamic lubrication of synovial joints. *Eng Med.* 1986;15:63–65.
8. Galvin AL, Tipper JL, Ingham E, Fisher J. Nanometre size wear debris generated from crosslinked and non-crosslinked ultra high molecular weight polyethylene in artificial joints. *Wear.* 2005;259: 977–983.
9. Glant TT, Jacobs JJ, Molnar G, Shanbhag AS, Valyon M, Galante JO. Bone resorption activity of particulate-stimulated macrophages. *J Bone Miner Res.* 1993;8:1071–1079.
10. Goater JJ, O'Keefe RJ, Rosier RN, Puzas JE, Schwarz EM. Efficacy of ex vivo OPG gene therapy in preventing wear debris induced osteolysis. *J Orthop Res.* 2002;20:169–173.
11. Green TR, Fisher J, Stone M, Wroblewski BM, Ingham E. Polyethylene particles of a 'critical size' are necessary for the induction of cytokines by macrophages in vitro. *Biomaterials.* 1998;19: 2297–2302.
12. Hills BA. Boundary lubrication in vivo. *Proc Inst Mech Eng [H].* 2000;214:83–94.
13. Hills BA, Butler BD. Surfactants identified in synovial fluid and their ability to act as boundary lubricants. *Ann Rheum Dis.* 1984; 43:641–648.
14. Inagaki K, O'Driscoll SW, Neale PG, Uchiyama E, Morrey BF, An KN. Importance of a radial head component in Sorbie unlinked total elbow arthroplasty. *Clin Orthop Relat Res.* 2002;400:123–131.
15. Ingram JH, Stone M, Fisher J, Ingham E. The influence of molecular weight, crosslinking and counterface roughness on TNF-alpha production by macrophages in response to ultra high molecular weight polyethylene particles. *Biomaterials.* 2004;25:3511–3522.
16. Ishihara K, Iwasaki Y, Ebihara S, Shindo Y, Nakabayashi N. Photoinduced graft polymerization of 2-methacryloyloxyethyl phosphorylcholine on polyethylene membrane surface for obtaining blood cell adhesion resistance. *Colloids Surf B Biointerfaces.* 2000; 18:325–335.
17. Ishihara K, Nomura H, Mihara T, Kurita K, Iwasaki Y, Nakabayashi N. Why do phospholipid polymers reduce protein adsorption? *J Biomed Mater Res.* 1998;39:323–330.
18. Ishihara K, Okazaki A, Negishi N, Shinohara I, Okano T, Kataoka K, Sakurai Y. Photo-induced change in wettability and binding ability of azoaromatic polymers. *J Appl Polym Sci.* 1982;27: 239–245.
19. Ishihara K, Shinozuka T, Hanazaki Y, Iwasaki Y, Nakabayashi N. Improvement of blood compatibility on cellulose hemodialysis membrane: IV. Phospholipid polymer bonded to the membrane surface. *J Biomater Sci Polym Ed.* 1999;10:271–282.
20. Ishihara K, Ueda T, Nakabayashi N. Preparation of phospholipid polymers and their properties as polymer hydrogel membrane. *Polym J.* 1990;22:355–360.
21. Jacobs JJ, Roebuck KA, Archibeck M, Hallab NJ, Glant TT. Osteolysis: basic science. *Clin Orthop Relat Res.* 2001;393:71–77.
22. Jono K, Takigawa Y, Takadama H, Mizuno M, Nakamura T. A multi-station hip joint simulator study and wear characterization of commercial hip endoprostheses. *Ceram Eng & Sci Proc.* 2003;24: 255–260.
23. Kihara S, Yamazaki K, Litwak KN, Litwak P, Kameneva MV, Ushiyama H, Tokuno T, Borzelleca DC, Umezu M, Tomioka J, Tagusari O, Akimoto T, Koyanag H, Kurosawa H, Kormos RL, Griffith BP. In vivo evaluation of a MPC polymer coated continuous flow left ventricular assist system. *Artif Organs.* 2003;27: 188–192.
24. Kirk TB, Wilson AS, Stachowiak GW. The morphology and composition of the superficial zone of mammalian articular cartilage. *J Orthop Rheumatol.* 1993;6:21–28.
25. Kurtz S, Mowat F, Ong K, Chan N, Lau E, Halpern M. Prevalence of primary and revision total hip and knee arthroplasty in the United States from 1990 through 2002. *J Bone Joint Surg.* 2005;87: 1487–1497.
26. Lewis AL, Furze JD, Small S, Robertson JD, Higgins BJ, Taylor S, Ricci DR. Long-term stability of a coronary stent coating post-implantation. *J Biomed Mater Res.* 2002;63:699–705.
27. Lewis AL, Tolhurst LA, Stratford PW. Analysis of a phosphorylcholine-based polymer coating on a coronary stent pre- and post-implantation. *Biomaterials.* 2002;23:1697–1706.
28. Livingston BJ, Chmell MJ, Spector M, Poss R. Complications of total hip arthroplasty associated with the use of an acetabular component with a Hylamer liner. *J Bone Joint Surg Am.* 1997;79: 1529–1538.
29. Mahomed NN, Barrett JA, Katz JN, Phillips CB, Losina E, Lew RA, Guadagnoli E, Harris WH, Poss R, Baron JA. Rates and outcomes of primary and revision total hip replacement in the United States medicare population. *J Bone Joint Surg Am.* 2003;85:27–32.
30. Maloney WJ, Smith RL, Schmalzried TP, Chiba J, Huene D, Rubash H. Isolation and characterization of wear particles generated in patients who have had failure of a hip arthroplasty without cement. *J Bone Joint Surg Am.* 1995;77:1301–1310.
31. McKellop H, Shen FW, DiMaio W, Lancaster JG. Wear of gamma-crosslinked polyethylene acetabular cups against roughened femoral balls. *Clin Orthop Relat Res.* 1999;369:73–82.
32. McKellop H, Shen FW, Lu B, Campbell P, Salovey R. Effect of sterilization method and other modifications on the wear resistance of acetabular cups made of ultra-high molecular weight polyethylene. A hip-simulator study. *J Bone Joint Surg Am.* 2000;82: 1708–1725.
33. Merx H, Dreinhofer K, Schrader P, Sturmer T, Puhl W, Gunther KP, Brenner H. International variation in hip replacement rates. *Ann Rheum Dis.* 2003;62:222–226.
34. Moro T, Takatori Y, Ishihara K, Konno T, Takigawa Y, Matsushita T, Chung UI, Nakamura K, Kawaguchi H. Surface grafting of artificial joints with a biocompatible polymer for preventing periprosthetic osteolysis. *Nat Mater.* 2004;3:829–836.
35. Muratoglu OK, Greenbaum ES, Bragdon CR, Jasty M, Freiberg AA, Harris WH. Surface analysis of early retrieved acetabular polyethylene liners: a comparison of conventional and highly crosslinked polyethylenes. *J Arthroplasty.* 2004;19:68–77.
36. Ogawa R, Iwasaki Y, Ishihara K. Thermal property and processability of elastomeric polymer alloy composed of segmented polyurethane and phospholipid polymer. *J Biomed Mater Res.* 2002;62: 214–221.
37. Older J. Charnley low-friction arthroplasty: a worldwide retrospective review at 15 to 20 years. *J Arthroplasty.* 2002;17:675–680.
38. Paul JP. Forces transmitted by joints in the human body. *Proc Inst Mech Eng [H].* 1967;181:8–15.
39. Shanbhag AS, Bailey HO, Hwang DS, Cha CW, Eror NG, Rubash HE. Quantitative analysis of ultrahigh molecular weight polyethylene (UHMWPE) wear debris associated with total knee replacements. *J Biomed Mater Res.* 2000;53:100–110.
40. Williams PF 3rd, Powell GL, LaBerge M. Sliding friction analysis of phosphatidylcholine as a boundary lubricant for articular cartilage. *Proc Inst Mech Eng [H].* 1993;207:59–66.
41. Wright TM, Rimnac CM, Faris PM, Bansal M. Analysis of surface damage in retrieved carbon fiber-reinforced and plain polyethylene tibial components from posterior stabilized total knee replacements. *J Bone Joint Surg Am.* 1988;70:1312–1319.
42. Yoneyama T, Sugihara K, Ishihara K, Iwasaki Y, Nakabayashi N. The vascular prosthesis without pseudointima prepared by antithrombogenic phospholipid polymer. *Biomaterials.* 2002;23: 1455–1459.

Eur Spine J (2006) 15: 1521–1528
DOI 10.1007/s00586-005-0005-8

ORIGINAL ARTICLE

Yu Koshizuka
Naoshi Ogata
Masataka Shiraki
Takayuki Hosoi
Atsushi Seichi
Katsushi Takeshita
Kozo Nakamura
Hiroshi Kawaguchi

Distinct association of gene polymorphisms of estrogen receptor and vitamin D receptor with lumbar spondylosis in post-menopausal women

Received: 29 April 2005
Revised: 21 August 2005
Accepted: 9 October 2005
Published online: 14 December 2005

Y. Koshizuka · N. Ogata · A. Seichi
K. Takeshita · K. Nakamura
H. Kawaguchi (✉)
Department of Orthopaedic Surgery,
Faculty of Medicine, University of Tokyo,
Hongo 7-3-1, Bunkyo-ku 113-8655, Tokyo,
Japan
E-mail: kawaguchi-ort@h.u-tokyo.ac.jp
Tel.: +81-3-58008656
Fax: +81-3-38184082

M. Shiraki
Research Institute and Practice
for Involutional Diseases,
Nagano, Japan

T. Hosoi
Tokyo Metropolitan Geriatric Hospital,
Tokyo, Japan

Abstract Contribution of genetic backgrounds to the etiology of lumbar spondylosis has been suggested by epidemiological studies. This study was designed to determine the association of restriction fragment length polymorphisms (RFLPs) of estrogen receptor (ER), vitamin D receptor (VDR), parathyroid hormone (PTH) and interleukin-1β (IL-1β) genes with the radiological severity of lumbar spondylosis at the disk level from L1/2 to L5/S1 in Japanese post-menopausal women. ER and VDR RFLP haplotypes were associated with the severity of spondylosis in the upper levels (L1/2 and L2/3) more than in the lower levels. Association of ER genotype was more pronounced in the group younger than average than in the older group, while that of VDR genotype was more significant in the older group. Neither PTH nor IL1-β RFLP was associated with the severity at any levels in either stratified group. We thus conclude that ER and VDR genes may contribute to lumbar spondylosis in a distinct manner: estrogen sensitivity influences the severity in the early phase after menopause while vitamin D plays an important role at older ages when the contribution of estrogen loss is weaker.

Keywords Spondylosis · Polymorphism · Estrogen receptor · Vitamin D receptor

Introduction

Osteoarthritis including spinal spondylosis, a chronic degenerative joint disorder, is prevalent in society as a major cause of disability. In Western countries, 10–50% of the senior population is affected by osteoarthritis, a quarter of whom are severely disabled due to joint symptoms or neuropathies [6]. In Japan as well, approximately 10 million of the country's 120 million inhabitants are suffering from osteoarthritis, with the figure increasing by 900,000 every year. Because of the prevalence of the disease in the elderly, this trend is occurring worldwide as a consequence of increasing longevity due to the overall improvement in living conditions and health status [21]. Despite significant social demand, research on osteoarthritis is still marginalized within biomedical research, so that the molecular and genetic bases for the disease are largely unmapped.

Family studies have suggested that not only osteoarthritis of the knee and hand [8, 14, 30], but also spinal spondylosis and degeneration [3, 27] have a strong genetic component with an increased prevalence in first-degree relatives of affected individuals. A twin study demonstrated a clear genetic effect for radiographic osteoarthritis of the knee and hand in women, with 39–65% of the variance being explained by genetic factors [30]. Recent population-based case-control studies have disclosed the association of polymorphisms of bone and cartilage metabolism regulatory factor

genes with common skeletal disorders, such as osteoporosis and osteoarthritis. These include genes for estrogen receptor (ER), vitamin D receptor (VDR), parathyroid hormone (PTH) and interleukin-1 (IL-1) [1, 2, 4, 5, 7, 10, 12, 15, 16, 19, 20, 22, 29, 33, 35, 36]. Several investigations have suggested polymorphisms in the genes encoding ER, VDR, type II procollagen, type XI collagen and transforming growth factor-β are associated with either the development or severity of osteoarthritis of extremities [1, 4, 16, 18, 33–35]. However, there are only a few reports on the association of gene polymorphisms with spinal spondylosis [36, 37]. Indeed, several factors including late onset of the disorder, lack of a large family suitable for genetic linkage analysis, a strong contribution of environmental factors, such as accumulated mechanical stress to the spine, and a probable polygenetic nature of the disease have hampered the genetic analysis of the disorder. Hence, this study focused on the association of polymorphisms of certain candidate genes: ER, VDR, PTH and IL-1β, all of which are known to be potent regulators of skeletal metabolism, with spondylotic changes of the lumbar spine in a population of Japanese postmenopausal women.

Materials and methods

Subjects

Genotype analyses were carried out using genomic DNA extracted from peripheral blood samples obtained from 318 post-menopausal Japanese women living in Nagano prefecture. All patients were unrelated volunteers who gave informed consent before the study. Since this is a rural area located in the central Japan with little change of inhabitants, the population in each generation shares similar genetic backgrounds from the Japanese typical ethnic ancestry as previously reported [28]. The number of samples for each gene analysis was different since the content of the informed consent varied depending on the time of the sample collection; that is, at the start of this project we stated only VDR genotyping analysis in the informed consent, and added ER, IL-1β, and PTH analyses in it thereafter. The clinical characteristics of the women recruited for the study were as follows: mean ± SD of age 63.7 ± 10.0 (range 51–76) years old, body height 151.0 ± 6.5 cm, body weight: 50.8 ± 8.0 kg, and body mass index (BMI) 22.3 ± 3.1 kg/m^2. Exclusion criteria included endocrinological disorders (e.g., hyperthyroidism, hyperparathyroidism, diabetes mellitus), liver or renal diseases, use of medications that were known to affect bone and cartilage metabolism (e.g., estrogen, bisphosphonates, vitamin D, calcium supplement, corticosteroids, anticonvulsants, heparin), and unusual gynecological history. The patients were also divided into two subpopulations, younger and older groups, bordered by the average age: 63.9 years for ER, 63.6 years for VDR, 63.7 years for PTH, and 64.1 years for IL-1β.

Measurements of phenotypes

The severity of spondylosis in the disk level from L1/2 to L5/S1 was graded according to the Kellgren–Lawrence scoring (grade 0–4) on a lateral radiograph of the lumbar spine under standardized conditions. This scoring is a well-known system for grading osteoarthritis severity of many joints [17], and has widely been used in previous studies to assess the severity of lumbar spondylosis [23, 38]. The scoring is designated as follows: 0 = normal; 1 = doubtful narrowing of joint space and possible osteophyte formation; 2 = definite osteophytes and possible narrowing of joint space; 3 = moderate multiple osteophytes, definite narrowing of joint space, some sclerosis, and possible deformity of bone contour; 4 = large osteophytes, marked narrowing of joint space, severe sclerosis, and definite deformity of bone contour. Bone mineral density (BMD, mg/cm^2) of the second through fourth lumbar spine (L2–L4) was measured by dual-energy X-ray absorptiometry (DPX-L, Lunar Co., Madison, WI). This parameter was expressed as a Z score that is a deviation from the weight-adjusted average BMD of each age based on the data of 20,000 Japanese women installed in Lunar DPX-L. The study protocol was approved by the ethical committee for human subjects of the University of Tokyo.

Genomic DNA analysis for restriction fragment length polymorphism

Genomic DNA (0.1 μg) was subjected to polymerase chain reaction (PCR) amplification using Taq DNA polymerase (PE Biosystem, Foster City, CA) with the sense and antisense primers synthesized by Operon Biotechnologies Inc. (Tokyo, Japan) upon request (Table 1). PCR products were digested by restriction endonucleases: *Pvu*-II and *Xba*-I for ER, *Apa*-I and *Bsm*-I for VDR, Bst-BI and *Dra*-I for PTH, and *Aba*-I for IL-1β, and digested products were analyzed by 1.2% agarose gel electrophoresis. The allele that could be digested by the enzyme was expressed by (+) while that could not by (−), and the RFLP genotype was expressed by the combination: ++, +−, and −−. In addition to the genotypes, the haplotypes were shown as the combination of two RFLP genotypes (++ = 1, +− = 2, and −− = 3) in ER (*Pvu*-II:*Xba*-I), VDR (*Apa*-I:*Bsm*-I) or PTH (*Bst*-BI:*Dra*-I) [11, 12, 13, 21, 22, 23, 31, 32, 33]. Hardy-Weinberg equilibrium [11] was used to determine whether or not there are large departures from independence between pairs of alleles at a gene locus.

Table 1 Primers for RFLP in each candidate gene

Gene	Forward	Reverse	Product size (bp)	Annealing temperature (°C)
ER	CTGCCACCCTATCTGTATCTTTC	TCTTTCTCTGCCACCCTGGCGTCG	629	57
VDR	AGCTGGCCCTGGCACTGACTC	ATGGAAACACCTTGCTTCTTCTCCC	265	56
PTH	CATTCTGTGTACTATAGTTTG	GAGCTTTGAATTAGCAGCATG	384	54
IL-1β	CTCATATTCCTGGCTAGTTTTGCTGA	TTGAAAGCACAGTCGGGCATAC	345	56

Linkage disequilibrium among these RFLPs was evaluated by calculating haplotype frequencies according to the method by Hill [13] and Thompson et al. [32].

Statistical analyses

Means of Kellgren–Lawrence score in each genotype or haplotype were evaluated by ANOVA and significance of differences was determined by post-hoc testing using Bonferroni's method. The χ^2 test was used to assess Hardy–Weinberg equilibrium. A P value less than 0.05 was considered statistically significant.

Results

Association of ER, VDR, PTH and IL-1β RFLP genotypes with lumbar spondylosis

Table 2 shows the background data of the study participants. The genotypic frequencies for these RFLPs were not significantly different in any subpopulation from those expected for populations in Hardy–Weinberg equilibrium (all $P > 0.05$). In addition, none of the linkage disequilibrium values for marker pairs differed significantly from zero (all $P > 0.05$), indicating there was no significant linkage disequilibrium among these RFLPs.

Regarding the association of the genotypes with the background data, no significant difference in age, body weight, height or BMI was seen among the RFLP genotypes in ER, VDR, PTH or IL-1β (all $P > 0.05$). BMD (L2–4) expressed as the Z score after being adjusted by age and weight also was not different among the genotypes.

When associations between the RFLP genotypes and the severity of spondylosis determined by the Kellgren–Lawrence grading were examined, there was no significant difference of the severity among genotypes in any RFLPs at any disk level from L1/2 to L5/S1 (all $P > 0.05$, data not shown). For a stratified analysis by age, we divided the population into two groups younger and older than the average age in each genotype popu-

Table 2 Background data of women of each genotype

Gene	Enzyme	Genotype	Age (years)	Body height (cm)	Body weight (kg)	BMI	BMD (Z score)
ER ($n=261$)	*Pvu*-II	++($n=78$)	63.1 (10.1)	150.3 (6.2)	49.9 (8.5)	22.0 (3.0)	0.121 (1.433)
		+−($n=139$)	64.2 (10.7)	150.8 (7.2)	50.6 (8.0)	22.3 (3.3)	−0.006 (1.432)
		−−($n=44$)	64.5 (9.0)	151.3 (6.3)	52.4 (7.9)	22.9 (2.8)	−0.259 (1.191)
	Xba-I	++($n=176$)	63.4 (10.8)	150.5 (6.7)	50.1 (8.3)	22.1 (2.9)	0.004 (1.427)
		+−($n=79$)	64.8 (8.9)	151.5 (6.9)	52.2 (7.9)	22.8 (3.5)	−0.037 (1.360)
		−−($n=6$)	66.7 (8.2)	147.3 (4.8)	48.7 (6.3)	22.4 (2.4)	−0.047 (1.179)
VDR ($n=318$)	*Apa*-I	++($n=125$)	63.3 (9.8)	151.0 (6.9)	51.4 (8.7)	22.5 (3.5)	−0.055 (1.498)
		+−($n=149$)	64.0 (10.1)	151.1 (6.0)	50.7 (7.6)	22.2 (2.8)	0.137 (1.463)
		−−($n=44$)	63.3 (10.1)	150.3 (6.5)	49.4 (6.8)	21.9 (2.7)	−0.332 (1.206)
	Bsm-I	++($n=238$)	63.6 (9.9)	151.1 (6.5)	51.0 (8.3)	22.3 (3.2)	0.059 (1.491)
		+−($n=72$)	64.0 (10.5)	150.7 (6.2)	50.5 (7.0)	22.2 (2.6)	−0.214 (1.325)
		−−($n=8$)	62.1 (8.0)	149.1 (5.9)	46.4 (6.0)	20.9 (3.1)	−0.489 (1.110)
PTH ($n=104$)	*Bst*-BI	++($n=1$)	60 (–)	153 (–)	39 (–)	16.7 (–)	−0.700 (–)
		+−($n=14$)	62.3 (12.6)	151.8 (7.2)	51.5 (7.4)	22.3 (2.9)	−0.576 (1.262)
		−−($n=89$)	63.9 (10.4)	150.3 (6.0)	50.5 (7.2)	22.4 (3.1)	−0.142 (1.335)
	Dra-I	++($n=0$)	–	–	–	–	–
		+−($n=27$)	63.2 (12.1)	150.0 (6.1)	50.0 (7.0)	22.2 (2.6)	−0.590 (1.314)
		−−($n=77$)	63.8 (10.1)	150.7 (6.2)	50.7 (7.4)	22.3 (3.2)	−0.071 (1.307)
IL-1β ($n=116$)	*Aba*-I	++($n=44$)	64.9 (10.9)	150.7 (7.1)	50.8 (7.9)	22.4 (3.4)	−0.395 (1.248)
		+−($n=52$)	63.8 (12.5)	151.3 (5.5)	50.1 (6.3)	21.9 (2.8)	−0.059 (1.282)
		−−($n=20$)	63.1 (9.7)	149.1 (5.1)	50.0 (8.2)	22.5 (3.3)	−0.318 (1.500)

Data of age, body height, weight, BMI, BMD (L2-4, Z score) are expressed by the mean (SD)

Table 3 Background data of women of each haplotype

Gene	Haplotype	Age (years)	Body height (cm)	Body weight (kg)	BMI	BMD (*Z* score)
ER ($n=261$) (*Pvu*-II: *Xba*-I)	11 ($n=5$)	69.6 (4.5)	147.0 (5.3)	47.6 (6.3)	22.0 (2.5)	0.224 (1.089)
	12 ($n=20$)	64.7 (8.1)	153.0 (6.1)	54.9 (9.5)	23.4 (3.3)	−0.470 (0.902)
	13 ($n=19$)	63.1 (10.5)	150.7 (6.4)	51.2 (5.4)	22.5 (2.2)	−0.159 (1.478)
	21 ($n=1$)	52 (–)	149 (–)	54 (–)	24.3 (–)	−0.601 (–)
	22 ($n=58$)	64.8 (9.3)	150.9 (7.2)	51.0 (7.0)	22.5 (3.5)	0.106 (1.476)
	23 ($n=80$)	63.8 (11.6)	150.7 (7.2)	50.3 (8.8)	22.1 (3.0)	−0.077 (1.413)
	32 ($n=1$)	62 (–)	158 (–)	65 (–)	26.0 (–)	0.800 (–)
	33 ($n=77$)	63.1 (10.1)	150.2 (6.2)	49.7 (8.3)	22.0 (3.0)	0.112 (1.441)
VDR ($n=318$) (*Apa*-I:*Bsm*-I)	11 ($n=7$)	61.9 (8.6)	149.1 (6.4)	45.9 (6.3)	20.7 (3.2)	−0.574 (1.170)
	12 ($n=16$)	62.8 (8.5)	152.3 (6.0)	52.9 (6.5)	23.1 (3.0)	−0.797 (1.242)
	13 ($n=21$)	64.0 (11.9)	150.0 (7.0)	48.0 (6.2)	21.3 (2.0)	0.124 (1.069)
	21 ($n=1$)	64 (–)	149 (–)	50 (–)	22.5 (–)	0.110 (–)
	22 ($n=56$)	64.3 (11.1)	150.5 (6.3)	49.8 (7.0)	21.9 (2.5)	−0.420 (1.310)
	23 ($n=91$)	63.8 (9.6)	151.3 (5.8)	51.2 (8.0)	22.3 (3.0)	0.246 (1.554)
	33 ($n=126$)	63.4 (9.8)	151.1 (7.0)	51.4 (8.7)	22.5 (3.5)	−0.850 (1.498)
PTH ($n=104$) (*Bst-Bl*:*Dra*-I)	11 ($n=64$)	63.7 (10.0)	150.7 (6.1)	50.8 (7.2)	22.4 (3.2)	0.001 (1.320)
	12 ($n=25$)	64.6 (11.5)	149.4 (5.8)	49.6 (7.2)	22.2 (2.7)	−0.509 (1.328)
	21 ($n=12$)	65.0 (11.4)	150.9 (7.3)	51.0 (7.4)	22.4 (3.1)	−0.325 (1.307)
	22 ($n=2$)	46.0 (1.4)	157.0 (5.7)	54.5 (2.1)	22.1 (0.7)	−1.600 (0.566)
	31 ($n=1$)	60 (–)	153 (–)	39 (–)	16.7 (–)	−0.700 (–)

Haplotypes are shown as the combination of two RFLP genotypes (+ + = 1, + − = 2, and − − = 3) in ER (*Pvu*-II:*Xba*-I), VDR (*Apa*-I:*Bsm*-I) or PTH (*Bst-Bl*:*Dra*-I). Data of age, body height, weight, BMI and BMD (L2-4, Z score) are expressed by the mean (SD)

lation. Here again, there was no significant association between RFLP genotypes and spondylosis severity at any levels in either population (data not shown).

Association of ER, VDR, PTH and IL-1β RFLP haplotypes with lumbar spondylosis

We further examined two RFLPs jointly in ER, VDR and PTH by haplotypic analysis. No significant difference in age, body weight, height, BMI or BMD (L2–4, *Z* score) was seen among the RFLP haplotypes in ER, VDR, PTH or IL-1β (Table 3, all $P > 0.05$). Association studies revealed that there were significant differences in the severity of spondylosis among haplotypes of ER (Fig. 1) and VDR (Fig. 2) RFLPs, especially in the upper levels of the lumbar spine (L1/2 and L2/3). A stratified analysis by age revealed that the association of the ER haplotype was more pronounced in the younger group (≤ 63.9 years) than in the older group (> 63.9 years). Contrarily, the association of the VDR haplotype was more significant in the older group (> 63.6 years) than in the younger group (≤ 63.6 years). The PTH RFLP haplotype was not associated with the severity at any level in either group.

Discussion

To learn the involvement of ER, VDR, PTH and IL-1β genes in the etiology of lumbar spondylosis in post-menopausal women, this study looked at the association between the polymorphisms and the severity of spondylosis. The RFLP haplotypes of ER and VDR, although not their genotypes, were associated with the spondylosis of the upper lumbar spine. It is well known that the spondylotic change occurs more frequently in the lower levels like L4/5 or L5/S1 than in the upper levels, and that the most important environmental factor for these disorders is the accumulation of mechanical stress. Hence, it is speculated that genetic contribution may be more prominent in the upper lumbar spine where the influence of the accumulating mechanical stress is relatively small.

Interestingly, the subpopulations in which ER and VDR showed significant associations with spondylosis were different: the former in younger and the latter in older subpopulations, suggesting that these two genes distinctly contribute to lumbar spondylosis. However, the mechanisms whereby the ER and VDR genes associated with the severity pose a risk for this condition are currently unclear. Although the present study did not investigate the association of these polymorphisms with osteoarthritis of the extremities, previous reports have strongly indicated that the present findings are not specific to lumbar spondylosis, but rather commonly seen in general osteoarthritic disorders. ER polymorphism may generally affect the estrogen sensitivity in the joint cartilage, which may influence the severity in the early phase after menopause. Involvement of estrogen in osteoarthritis and spondylosis is consistent with the larger increases in women than in men in the prevalence of the disorder after 50 years of age, and actually, two estrogen

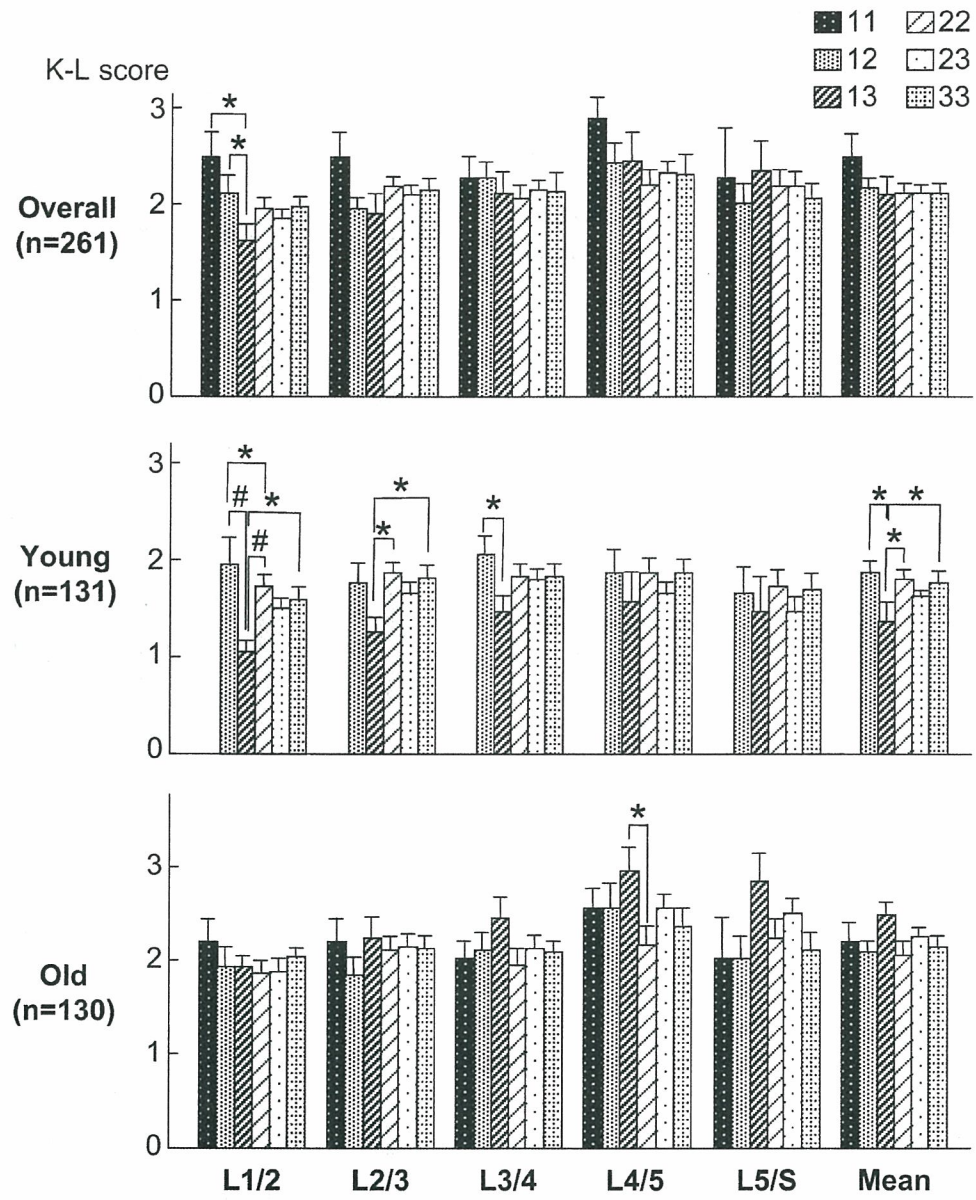

Fig. 1 Association between ER RFLP haplotypes and the severity of spondylosis at disk levels (L1/2-L5/S1) in the overall ($n=261$), younger ($n=131$) and older ($n=130$) populations of post-menopausal women. The allele that could be digested by *Pvu*-II and *Xba*-I endonucleases was expressed by (+) while that which could not by (−), and the genotype was shown by the combination: ++ = 1, +− = 2, and −− = 3. The haplotypes were further expressed by the combination of genotypes (11, 12, 13, 21, 22, 23, 31, 32, 33). The severity of spondylosis at each disk level was graded according to the Kellgren–Lawrence score (grade 0–4) on a lateral radiograph of the lumbar spine. Patients were divided into two subpopulations younger and older than the average age: 63.6 years. Data are expressed as means (*bars*) ± SEMs (*error bars*). $*P<0.05$, $\#P<0.01$; significant difference

receptors (ERα and ERβ) have been identified in normal and osteoarthritic cartilage [26, 35], indicating that the cartilage can respond to estrogen. Furthermore, hormone replacement therapy for menopause seems to be associated with a decrease in the prevalence of symptoms and radiological alterations related to osteoarthritis [25]. Estrogen can influence chondrocyte function on multiple levels by interacting with cellular growth factors, adhesion molecules and cytokines. Nevertheless, findings regarding the correlation between estrogen and osteoarthritis are inconsistent and inconclusive and range from estrogen protecting against osteoarthritis to cartilage damage mediated by high levels of estrogen and higher binding to estrogen receptors [9]. Contrary to estrogen, vitamin D may play an important role in spondylosis at older ages when the contribution of estrogen loss is weaker. Expression of vitamin D receptor has also been detected in osteoarthritic cartilage and human articular chondrocytes; however, its function on chondrocytes is unclear [31]. Indeed, the present and previous studies could implicate the VDR gene itself to be functionally involved in the etiology of osteoarthritis [16, 33, 36].

Alternatively, since there are a number of reports indicating that ER and VDR genotypes are implicated in determining bone density [2, 7, 12, 19, 20, 22], the

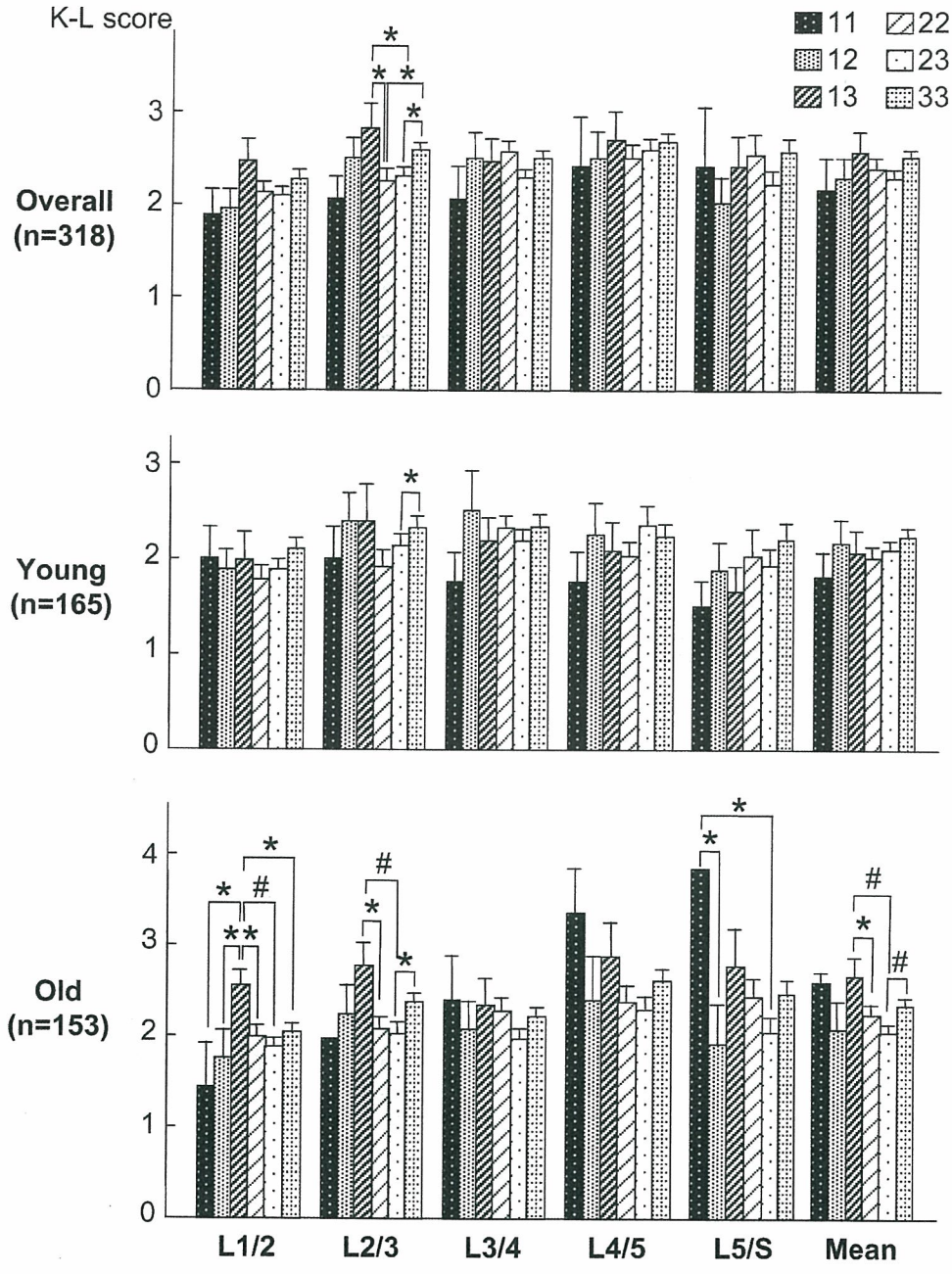

Fig. 2 Association between VDR RFLP haplotypes and the severity of spondylosis at disk levels (L1/2-L5/S1) in the overall ($n=318$), younger ($n=165$) and older ($n=153$) populations of postmenopausal women. The haplotypes were expressed by the combination of RFLP genotypes by *Apa*-I and *Bsm*-I endonuclease digestions as described in Fig. 1. The severity of spondylosis at each disk level was graded according to the Kellgren–Lawrence score (grade 0–4) on a lateral radiograph of the lumbar spine. Patients were divided into two subpopulations younger and older than the average age: 63.9 years. Data are expressed as means (*bars*) ± SEMs (*error bars*). $*P<0.05$, $\#P<0.01$; significant difference

significant association between the RFLPs and spondylosis might be secondary to the effects on bone density. This would be in line with the suggestion that decreased bone density could lead to less damage of articular cartilage because of differential impact loading [24]. In the present study, however, the fact that there was no difference in bone density among the RFLP genotypes and haplotypes (Tables 2, 3) indicates that the findings on spondylosis are independent of bone density in the lumbar spine.

Considering that neither of the ER and VDR polymorphic sites is located in exons but instead in introns, these nucleotide variants do not directly lead to amino acid substitutions. The most likely mechanism may be that these intronic substitutions affect the splicing mechanism; the one base substitution may yield an alternate transcript with abnormal function or affect the expression level of proteins. The next task ahead of us will be to investigate the relevance of these polymorphisms to the production or function of ER and VDR.

Regarding the clinical utility of this study, the practical application of this genetic information of individuals to specific diagnostic or therapeutic modifications is a conceptual goal. It is true that the ER and VDR gene polymorphisms might possibly be useful diagnostic markers to predict the progression of lumbar spondylosis; however, this study demonstrated no more than the possible involvement of ER and VDR signalings in this disorder, and is incomplete and premature for clinical use. For example, the cut-off between 'young' and 'old' is the average age of the population just happened to be enrolled in the present study, but not a definite age that is applicable to the general population. Our stratified analysis to decide the cut-off age by dividing the population into five generations: <56, 56–60, 61–65, 66–70, and >70, failed to show the clear association of ER or VDR polymorphism with the lumbar spondylosis (data not shown). This may be at least partly due to the insufficiency of the population in each subgroup, which results in significant difference ($P<0.05$) of the genotypic frequencies from those expected in Hardy–Weinberg equilibrium in the subpopulations. To decide the cut-off age for the exact diagnostic criteria by the ER and VDR polymorphisms, it will be essential to increase the population studied, so that more precise stratified analyses can be done. In addition, although the objective of this study is limited to post-menopausal women, the conclusion will be more enhanced with the inclusion of other ages like premenopausal women. Regarding therapeutic modifications, estrogen and vitamin D themselves or regulators of their expressions or functions might possibly lead to conservative treatment to prevent the progression. In reality, however, such modification is an era away from the current generation. The legal, social, and ethical implications of this information are also overwhelming.

Using the information gained, we demonstrated possible associations of ER and VDR genes with lumbar spondylosis. These genes might have a relatively small attributable risk fraction for this disease; however, identification of the disease-susceptibility and disease - severity gene could lead to a better understanding of the molecular pathogenesis of the condition, which is essential to develop a significant diagnosis and treatment. Further studies on the functional relevance of these gene abnormalities could provide new biological insights into the etiology of diseases with osteoarthritis including spondylosis.

Acknowledgements This work was supported by a Grants-in-Aid for Scientific Research from the Japanese Ministry of Education, Culture, Sports, Science and Technology (#15209049).

References

1. Ala-Kokko L, Baldwin CT, Moskowitz RW, Prockop DJ (1990) Single base mutation in the type II procollagen gene (COL2A1) as a cause of primary osteoarthritis associated with a mild chondrodysplasia. Proc Natl Acad Sci USA 87:6565–6568
2. Albagha OM, McGuigan FE, Reid DM, Ralston SH (2001) Estrogen receptor alpha gene polymorphisms and bone mineral density: haplotype analysis in women from the United Kingdom. J Bone Miner Res 16:128–134
3. Battie MC, Videman T, Gibbons LE (1995) Determinants of lumbar disc degeneration. A study relating lifetime exposures and magnetic resonance imaging findings in identical twins. Spine 20:2601–2612
4. Bergink AP, van Meurs JB, Loughlin J (2003) Estrogen receptor alpha gene haplotype is associated with radiographic osteoarthritis of the knee in elderly men and women. Arthritis Rheum 48:1913–1922
5. Cattabriga M, Rotundo R, Muzzi L (2001) Retrospective evaluation of the influence of the interleukin-1 genotype on radiographic bone levels in treated periodontal patients over 10 years. J Periodontol 72:767–773
6. Doherty M (2001) Risk factors for progression of knee osteoarthritis. Lancet 358:775–776
7. Eisman JA (1995) Vitamin D receptor gene alleles and osteoporosis: an affirmative view. J Bone Miner Res 10:1289–1293
8. Felson DT, Couropmitree NN, Chaisson CE (1998) Evidence for a Mendelian gene in a segregation analysis of generalized radiographic osteoarthritis: the Framingham Study. Arthritis Rheum 41:1064–1071
9. Gokhale JA, Frenkel SR, Dicesare PE (2004) Estrogen and osteoarthritis. Am J Orthop 33:71–80
10. Gong G, Johnson ML, Barger-Lux MJ, Heaney RP (1999) Association of bone dimensions with a parathyroid hormone gene polymorphism in women. Osteoporos Int 9:307–311
11. Hardy GH (1908) Mendelian proportions in a mixed population. Science 28:49–50
12. Harris SS, Eccleshall TR, Gross C, Dawson-Hughes B, Feldman D (1997) The vitamin D receptor start codon polymorphism (FokI) and bone mineral density in premenopausal American black and white women. J Bone Miner Res 12:1043–1048
13. Hill WG (1974) Estimation of linkage disequilibrium in randomly mating populations. Heredity 33:229–239
14. Hirsch R, Lethbridge-Cejku M, Hanson R (1998) Familial aggregation of osteoarthritis: data from the Baltimore longitudinal study on aging. Arthritis Rheum 41:1227–1232
15. Hosoi T, Miyao M, Inoue S (1999) Association study of parathyroid hormone gene polymorphism and bone mineral density in Japanese postmenopausal women. Calcif Tissue Int 64:205–208
16. Keen RW, Hart DJ, Lanchbury JS, Spector TD (1997) Association of early osteoarthritis of the knee with a Taq I polymorphism of the vitamin D receptor gene. Arthritis Rheum 40:1444–1449

17. Kellgren JH, Lawrence JS (1957) Radiological assessment of osteoarthritis. Ann Rheum Dis 16: 494–501
18. Knowlton RG, Katzenstein PL, Moskowitz RW (1990) Genetic linkage of a polymorphism in the type II procollagen gene (COL2A1) to primary osteoarthritis associated with mild chondrodysplasia. N Engl J Med 322:526–530
19. Kobayashi S, Inoue S, Hosoi T, Ouchi Y, Shiraki M, Orimo H (1996) Association of bone mineral density with polymorphism of the estrogen receptor gene. J Bone Miner Res 11:306–311
20. Lau EM, Young RP, Lam V, Li M, Woo J (2001) Estrogen receptor gene polymorphism and bone mineral density in postmenopausal Chinese women. Bone 29:96–98
21. Mollenhauer JA, Erdmann S (2002) Molecular and biomechanical basis of osteoarthritis. Cell Mol Life Sci 59:3–4
22. Morrison NA, Qi JC, Tokita A (1994) Prediction of bone density by vitamin D receptor alleles. Nature 367:284–287
23. Muraki S, Yamamoto S, Ishibashi H, Horiuchi T, Hosoi T, Orimo H, Nakamura K (2004) Impact of degenerative spinal diseases on bone mineral density of the lumbar spine in elderly women. Osteoporos Int 15:724–728
24. Radin EL (1976) Mechanical aspects of osteoarthritis. Bull Rheum Dis 26:862–865
25. Richette P, Corvol M, Bardin T (2003) Estrogens, cartilage, and osteoarthritis. J Bone Spine 70:257–262
26. Richmond RS, Carlson CS, Register TC (2000) Functional estrogen receptors in adult articular cartilage: estrogen replacement therapy increases chondrocyte synthesis of proteoglycans and insulin-like growth factor binding protein 2. Arthritis Rheum 43:2081–2090
27. Sambrook PN, MacGregor AJ, Spector TD (1994) Genetic influences on cervical and lumbar disc degeneration: a magnetic resonance imaging study in twins. Arthritis Rheum 42:366–372
28. Shiraki M, Shiraki Y, Aoki C, Hosoi T, Inoue S, Kaneki M, Ouchi Y (1997) Association of bone mineral density with apolipoprotein E phenotype. J Bone Miner Res 12:1438–1445
29. Silver A, Boultwood J, Breckon G (1989) Interleukin-1 beta gene deregulation associated with chromosomal rearrangement: a candidate initiating event for murine radiation-myeloid leukemogenesis. Mol Carcinog 2:226–232
30. Spector TD, Cicuttini F, Baker J (1996) Genetic influences on osteoarthritis in women: a twin study. Br Med J 312:940–943
31. Tetlow LC, Woolley DE (2001) Expression of vitamin D receptors and matrix metalloproteinases in osteoarthritic cartilage and human articular chondrocytes in vitro. Osteoarthritis Cartilage 9:423–431
32. Thompson EA, Deeb S, Walker D, Motulsky AG (1998) The detection of linkage disequilibrium between closely linked markers: RFLPs at the AI-CIII apolipoprotein genes. Am J Hum Genet 42:113–124
33. Uitterlinden AG, Burger H, Huang QJ Odding E, Duijn CM, Hofman A, Birkenhager JC, van Leeuwen JP, Pols HA (1997) Vitamin D receptor genotype is associated with radiographic osteoarthritis at the knee. J Clin Invest 100:259–263
34. Ushiyama T, Ueyama H, Inoue K Nishioka J, Ohkubo I, Hukuda S. (1998) Estrogen receptor gene polymorphism and generalized osteoarthritis. J Rheumatol 25:134–137
35. Ushiyama T, Ueyama H, Inoue K, Ohkubo I, Hukuda S (1999) Expression of genes for estrogen receptors alpha and beta in human articular chondrocytes. Osteoarthritis Cartilage 7:560–566
36. Videman T, Gibbons LE, Battie MC, Maravilla K, Vanninen E, Leppavuori J, Kaprio J, Peltonen L (2001) The relative roles of intragenic polymorphisms of the vitamin D receptor gene in lumbar spine degeneration and bone density. Spine 26:E7–12
37. Yamada Y, Okuizumi H, Miyauchi A, Takagi Y, Ikeda K, Harada A (2000) Association of transforming growth factor beta1 genotype with spinal osteophytosis in Japanese women. Arthritis Rheum 43:452–460
38. Yoshimura N, Dennison E, Wilman C, Hashimoto T, Cooper C (2000) Epidemiology of chronic disc degeneration and osteoarthritis of the lumbar spine in Britain and Japan: a comparative study. J Rheumatol 27:429–433

Exp. Anim. 55(4), 333–342, 2006

Therapeutic Effect of Risedronate on Cancellous and Cortical Bone in Ovariectomized Osteopenic Rats: A Comparison with the Effects of Alfacalcidol

Jun IWAMOTO[1)], Azusa SEKI[2)], Tsuyoshi TAKEDA[1)], Yoshihiro SATO[3)], Harumoto YAMADA[4)], and James K. YEH[5)]

[1)]*Department of Sports Medicine, Keio University School of Medicine, 35 Shinanomachi, Shinjuku-ku, Tokyo, 160-8582,* [2)]*Hamri Co., Ltd., Tokyo,* [3)]*Department of Neurology, Mitate Hospital, Fukuoka,* [4)]*Department of Orthopaedic Surgery, Fujita Health University, Aichi, Japan, and* [5)]*Metabolism Laboratory, Department of Medicine, Winthrop-University Hospital, NY, USA*

Abstract: *The purpose of the present study was to compare the therapeutic effects of risedronate (RIS) and alfacalcidol (ALF) on cancellous and cortical bone in ovariectomized osteopenic rats. Forty-two female Sprague-Dawley rats, 7 months of age, were randomized by the stratified weight method into six groups: the sham-operated control (Sham) group, and five ovariectomized groups: treated with vehicle, RIS (0.1, 1.0, or 2.5 mg/kg, p.o., daily), and ALF (0.5 μg/kg, p.o., daily). Treatment was started 6 weeks after surgery and continued for 6 weeks. Evaluation at 12 weeks after surgery revealed that ovariectomy (OVX) decreased the cancellous bone volume/total tissue volume (BV/TV) of the proximal tibial metaphysis as a result of an increase of the bone formation rate/bone surface (BFR/BS), BFR/BV, and eroded surface (ES/BS), while having no effect on the cortical area (Ct Ar) of the tibial diaphysis. OVX also decreased the maximum load of the femoral distal metaphysis, while having no effect on any mechanical property parameters of the femoral diaphysis. RIS (at all the doses) increased the BV/TV relative to the value in the OVX-Vehicle group, but the value was not restored to that observed in the Sham group. The effects of RIS (1.0 mg/kg and 2.5 mg/kg) were similar, and greater than those of RIS (0.1 mg/kg). ALF also increased the BV/TV relative to the OVX-Vehicle group, but the value was not restored to that observed in the Sham group, similar to the results of RIS (1.0 mg/kg and 2.5 mg/kg) treatment. The alterations of the structural parameters induced by RIS (at the doses) were attributable to suppression of the increase of ES/BS, BFR/BS, and BFR/BV. The alterations of the structural parameters induced by ALF were attributable to suppression of the increase of ES/BS and attenuation of the increase of BFR/BV, while the BFR/BS was maintained. ALF also increased the Ct Ar to beyond the value observed in the Sham group. RIS (at all the doses) had no effect on the mechanical properties of the femoral distal metaphysis, whereas ALF prevented the loss of the maximum load of the femoral distal metaphysis. Thus, the results of the present study show differential effects of RIS and ALF on cancellous and cortical bone in ovariectomized osteopenic rats.*

Key words: *alfacalcidol, osteopenia, ovariectomy, rat, risedronate,*

(Received 24 November 2005 / Accepted 3 February 2006)

Address corresponding: J. Iwamoto, Department of Sports Medicine, Keio University School of Medicine, 35 Shinanomachi, Shinjuku-ku, Tokyo 160-8582, Japan

Introduction

Osteoporosis is recognized as a major public health problem. Because estrogen deficiency associated with menopause causes marked bone loss, osteoporosis primarily affects postmenopausal women. The bisphosphonate, risedronate (RIS) and the active vitamin D_3, alfacalcidol (ALF), have been widely used for postmenopausal osteoporosis in Japan. Several large randomized controlled trials (RCTs) have demonstrated that RIS reduces the incidence of vertebral and hip fractures in postmenopausal osteoporotic women [7, 8, 12]. However, because no large RCTs have been conducted to determine the anti-fracture efficacy of ALF in postmenopausal osteoporotic women, its efficacy in the treatment of postmenopausal osteoporosis remains to be established.

Several preclinical studies have reported on the effects of RIS and ALF against cancellous osteopenia using a rat model of postmenopausal osteoporosis (the preventive effects of RIS and ALF on osteopenia) [6, 15, 20]. RIS suppresses bone resorption and prevents cancellous bone loss in ovariectomized rats [6, 15]. On the other hand, ALF suppresses bone resorption, but maintains or even stimulates bone formation, thereby increasing the bone mineral density (BMD) and improving the mechanical properties of the bone [20]. However, very few studies have reported on the therapeutic effects of RIS or ALF on the bone mass and mechanical properties in ovariectomized osteopenic rats (the therapeutic effects of RIS and ALF on established osteopenia). The purpose of the present study was to compare the therapeutic effects of RIS and ALF on cancellous and cortical bone in ovariectomized osteopenic rats.

Materials and Methods

Treatment of animals

Forty-two female Sprague-Dawley rats, 7 months of age, were purchased from Charles River Japan (Kanagawa, Japan). They were fed a pelleted standard chow diet containing 1.25% calcium and 0.9% phosphorus (CRF-1: Oriental Kobo, Co., Ltd., Tokyo, Japan). The animals were housed under local vivarium conditions (temperature 23.3°C, humidity 55%, and 12 h on/off light cycle), with free access to water. After allowing one week for adaptation to the new environment, the rats were randomized by the stratified weight method into the following six groups: sham-operation + vehicle (Sham, n=5) group, bilateral ovariectomy (OVX, n=5) + vehicle group, OVX + RIS (0.1 mg/kg [n=8], 1.0 mg/kg [n=8], and 2.5 mg/kg [n=8]) groups, and OVX + ALF (0.5 μg/kg, n=8) group. The treatment with vehicle, RIS, or ALF was started 6 weeks after surgery and continued for 6 weeks. Bilateral OVX was performed under general anesthesia induced by intraperitoneal injection of 25–30 mg/kg pentobarbital sodium. Tablet forms of RIS (Actonel, Aventis Pharma, Tokyo, Japan) or ALF (One-alfa, Teijin Pharma, Tokyo, Japan) were pulverized, dissolved in 0.1 ml of sterile saline, and administered orally to the animals daily by gavage deep into the mouth. The doses of RIS and ALF were determined based on the results of previous studies [6, 13, 15, 20]; the daily dose of ALF (0.5 μg/kg) was 5 times higher than the effective daily dose (0.1 μg/kg) for preventing the loss of the proximal, middle, and distal femoral BMD in OVX rats [20], while the daily doses of RIS, 0.1 mg/kg, 1.0 mg/kg, and 2.5 mg/kg were within the range of doses previously tested in OVX or hind-limb immobilized rats [6, 13, 15]. The skeletal efficacy of ALF in ovariectomized rats has clearly been established [20]. Because the present study focused on investigating the effect of RIS on established osteopenia after OVX and comparing the skeletal efficacy between RIS and ALF, the highly effective dose of ALF and the low, middle, and high dose of RIS were selected. Only vehicle (0.1 ml of sterile saline) was also administered orally to the animals daily by gavage in the Sham-vehicle and OVX-vehicle groups. The body weight of the rats was monitored weekly, and the total duration of the experiment was 12 weeks. The present study was carried out at the laboratory of Hamri Co., Ltd. (Ibaraki, Japan). The animals were maintained according to the National Institutes of Health (NIH) Guide for Care and Use of Laboratory Animals, and the animal experiment protocols were approved by the Laboratory Animal Care Committee of Hamri Co., Ltd. (Ibaraki, Japan).

Preparation of specimens

Urine samples from all the rats were collected over a 24 h period using metabolic cages 6, 9, and 12 weeks after the start of the experiment, and the specimens

were stored at –20°C. All the rats were labeled with 25 mg/kg of tetracycline (Sigma Chemical, St. Louis, MO, USA) injected intramuscularly and 8 mg/kg of calcein (Sigma Chemical, St. Louis, MO, USA) injected subcutaneously, 9 days and 3 days, respectively, before sacrifice. The animals were sacrificed 12 weeks after the surgery by exsanguination under anesthesia induced by intraperitoneal injection of 25–30 mg/kg of pentobarbital sodium. Upon sacrifice, serum specimens were collected from all the rats, and the right femur and right tibia were isolated.

The serum samples were stored at –20°C. The urine and serum samples were used for the measurements of biochemical markers as described below. The femurs were stored at –20°C and then used for biomechanical testing as described below. The tibiae were processed for bone histomorphometric analyses. The bones were fixed in cold 40% ethanol overnight, and then cut into three parts using an Isomet saw (Buehler, Lake Bluff, IL, USA). The proximal tibial metaphysis and tibial diaphysis with the fibular junction were stained with Villanueva Osteochrome Bone Stain (Polyscience, Warrington, PA, USA) for 5 days. The specimens were dehydrated sequentially in ascending concentrations of ethanol (70%, 95%, and 100%) and xylene, and then embedded in methyl-methacrylate (EM Science, Gibbstown, NJ, USA) at 4°C according to the method of Erben [5]. Cross-sections of the tibial diaphysis just proximal to the tibio-fibular junction were cut at 40 μm thickness using a diamond wire Histo-Saw machine (Delaware Diamond Knives, Wilmington, DE, USA), and the thickness of each cross-sectional specimen was determined with an Inspectors' Dial Bench Gauge (L.S. Starrett, Athol, MA, USA). Frontal sections of the proximal tibial metaphysis were cut at 8 μm or 4 μm thickness using a microtome (Leica RM2155; Leica Inc., Nussloch, Germany). The 8 μm sections were then transferred onto chromalum-gelatin-coated slides and dried overnight under a press at 42°C. All the sections were coverslipped with Eukitt (Calibrated Instruments, Hawthorne, NY, USA) for the static and dynamic histomorphometric analyses. For tartrate-resistant acid phosphatase (TRAP) histochemistry, the 8-μm sections of the proximal tibial metaphysis were deplasticized with three changes of 2-methoxyethylacetate for 30 min each, two changes of acetone for 5 min each, and sequential changes of ethanol (95%, 70%, and 40%), followed by two changes of deionized water for 5 min each for rehydration. The deplasticized and rehydrated sections (8 μm thickness) were placed in 0.1 M acetate buffer at pH 5.0 for 5 min, and the TRAP reaction was performed using a leukocyte acid phosphatase kit (Sigma Chemical, St. Louis, MO, USA). Sections stained for TRAP were counterstained with Mayer's hematoxylin (1 min) and then air-dried and mounted with a plastic UV mounting medium (Polysciences Inc., Warrington, PA, USA). For Goldner Trichrom staining to count the osteoblast surface, adjacent 4-μm sections of the proximal tibia metaphysis were deplasticized and rehydrated, followed by the procedure of Goldner Trichrom stain and mounting with Eukitt (Calibrated Instruments, Hawthorne, NY, USA).

Urine and serum biochemical analyses

The levels of urinary deoxypyridinoline (DPD) as a bone resorption marker were measured by enzyme-immunoassay (EIA) using a Pyrilinks-D kit (Metra Biosystems Inc., CA, USA). The serum calcium and phosphorus levels were measured by the o-CPC and ammonium molybdate colorimetric methods, respectively, using an autoanalyzer (Dada Behring Model RXL, Bakersfield, CA, USA). The levels of serum osteocalcin (OC) as a bone formation marker were measured by immunoradiometric assay (IRMA) using a Rat Osteocalcin IRMA kit (Immutopics, Inc., CA, USA).

Biomechanical testing

The mechanical properties of the diaphysis of the femur were evaluated by the three-point bending test. Load was applied midway between two supports placed 15 mm apart on the bone. The femur was positioned so that the loading point was at the center of the femoral diaphysis and bending occurred about the medial-lateral axis. The specimens were tested in a saline bath at 37°C. Each specimen was submerged in the saline bath for about 3 min before testing, to allow temperature equilibration. Load-displacement curves were recorded at a crosshead speed of 20 mm/min using a materials-testing machine (MZ500D; Maruto, Co., Ltd., Tokyo, Japan). The parameters analyzed were the maximum load, stiffness, and breaking energy.

Immediately after the three-point bending test of the right femoral diaphysis, the distal metaphysis was isolated over a length of 10 mm from the joint surface of

the femoral condyle. The mechanical properties of this segment were then measured by the compression test. Compressive load was applied by the rectangular parallelepiped crosshead (length 2 cm, width 2 cm, and height 1 cm) on the specimens from the lateral to the medial aspect. The specimens were tested in a saline bath at 37°C. Each specimen was submerged in the saline bath for about 3 min before testing, to allow temperature equilibration. Load-displacement curves were recorded at a crosshead speed of 10 mm/min and compression depth of 2.5 mm, using a materials-testing machine (MZ500D; Maruto, Co., Ltd., Tokyo, Japan). The parameters analyzed were the maximum load, stiffness, and breaking energy.

Bone histomorphometry of the tibia

A digitizing morphometry system was used to measure the bone histomorphometric parameters of the tibial specimens. The system consisted of an epifluorescence microscope (Nikon E-400, OsteoMetrics, Atlanta, GA, USA), an Osteomeasure High Resolution Color Subsystem (OsteoMetrics, Atlanta, GA, USA), and a digitizing pad (Numonics 2206; Numonics Corp., Montomerville, PA, USA) coupled to an IBM computer, and a morphometry program (OsteoMetrics, Atlanta, GA, USA). The measured parameters for cancellous bone included the total tissue volume (TV), bone volume (BV), bone surface (BS), eroded surface (ES), single- and double-labeled surfaces (sLS and dLS, respectively), and osteoblast surface (ObS). These data were used to calculate the percent cancellous bone volume (BV/TV), trabecular number (Tb N), trabecular thickness (Tb Th), trabecular separation (Tb Sp), ES/BS, MS/BS [(sLS/2+dLS)/BS], mineral apposition rate (MAR), bone formation rate (BFR)/BS, BFR/BV, and ObS/BS, in accordance with the standard nomenclature described by Parfitt *et al.* [16]. In the present study, the region of cancellous bone measured was 1–4 mm distal to the lower margin of the growth plate in the proximal tibia, which consists of secondary spongiosa. Cells showing positive staining for TRAP were counted in the region extending from the distal end of the growth plate to 0.2 mm from the growth plate, and the number of osteoclasts (N.Oc) and the osteoclast surface (OcS) per BS were calculated. The measured parameters for cortical bone were the total tissue area (Tt Ar), cortical bone area (Ct Ar), endocortical ES, periosteal and endocortical BS, sLS, dLS, and the interlabel width. These data were used to calculate the marrow area (Ma Ar), endocortical ES/BS, and periosteal and endocortical MS/BS [(sLS/2+dLS)/BS], MAR, and BFR/BS.

Statistical analysis

All the data were expressed as means and standard deviation (SD). Multiple comparisons of data among the groups were performed by analysis of variance (ANOVA) with Fisher's protected least significant difference (PLSD) test. All statistical analyses were performed using the Stat View J-5.0 program on a Macintosh computer. A significance level of $P<0.05$ was used for all the comparisons.

Results

Changes in body weight (Table 1)

The body weight at surgery did not differ significantly among the six groups. OVX was associated with an increase in the body weight of the animals. Neither RIS nor ALF affected the body weight of the ovariectomized animals.

Biochemical markers (Table 2)

OVX increased the urinary DPD and serum OC levels. RIS (at all the doses) decreased the serum phosphorus levels with the greatest decrease by RIS (2.5 mg/kg), while serum calcium levels were only decreased by RIS (2.5 mg/kg). RIS (1.0 mg/kg and 2.5 mg/kg) prevented the elevation of both the serum OC and urinary DPD levels, however, RIS (0.1 mg/kg) only attenuated the increase of the urinary DPD levels. A greater decrease of the serum OC levels was observed in the RIS (2.5 mg/kg) group than in the RIS (1.0 mg/kg) group. On the other hand, ALF mildly prevented the elevation of both the markers, without inducing any significant hypercalcemia.

Bone histomorphometric analysis of the cancellous bone of the proximal tibial metaphysis (Fig. 1 and Table 3)

The cancellous BV/TV, Tb N, and Tb Th were decreased, and the Tb Sp was increased, 12 weeks after OVX, as a result of increased bone resorption (ES/BS, N.Oc/BS, OcS/BS) and bone formation (ObS/BS, MS/BBS, BFR/BS, BFR/BV). RIS (at all the doses) increased the BV/TV, Tb N, and decreased the Tb Sp